Axion and ALP couplings at quantum level

Jesús Bonilla García

Máster en Física Teórica

MÁSTERES DE LA UAM

2018 - 2019

Facultad de Ciencias

UAM Universidad Autónoma de Madrid

Universidad Autónoma de Madrid

Master Thesis

Axion and ALP couplings at quantum level

Jesús Bonilla García

Supervisors: Prof. Belén Gavela Legazpi and Pablo Quílez Lasanta

Abstract

In this work we review the Strong CP problem of the Standard Model, we derive novel one-loop amplitudes for axion and axion-like-particle coupling and, furthermore, new bounds on the parameter space for axion and axion-like-particle are derived. Axions are studied as a solution to the Strong CP problem, presenting several axion models such as the original Peccei-Quinn-Weinberg-Wilczek axion, invisible axion models and heavy axion models. The main axion detection experiments are also reviewed, as well as the standard constraints on the parameter space of the axion. Additionally, we explain a novel approach that is being considered in the search of axion and axion-like-particles, called non-resonant searches, and use it to establish a new constraint on the effective coupling of the axion to charged leptons. In order to do this, the loop-induced coupling of the axion to photons induced by leptons is computed and applied for the first time to non-resonant searches.

CONTENTS

1 **Introduction** **1**

2 **Strong CP problem** **5**

2.1 Instantons in QCD 5

2.2 The ABJ anomaly 7

2.3 Neutron electric dipole moment 12

3 **Peccei-Quinn solutions to the Strong CP problem: the axion** **16**

3.1 Massless fermions with colour charge 16

3.2 Peccei-Quinn-Weinberg-Wilczek axion 17

3.3 Invisible axion models 19

3.3.1 DFSZ axion 19

3.3.2 KSVZ axion 20

3.4 Heavy axion models 21

4 **Effective Lagrangian for axions and ALPs** **23**

4.1 Effective couplings to vector bosons 23

4.2 Loop-induced couplings 29

4.3 New constraints: non-resonant searches 35

5 **Conclusions** **41**

Acknowledgements **42**

References **43**

1. INTRODUCTION

The Standard Model of particle physics (SM) is a theory that describes with great precision three out of the four fundamental forces of the nature, through which all the known particles interact. Nevertheless, we have observed some phenomena that seem to require the existence of new particle physics beyond SM (BSM), such as neutrino oscillations or the nature of dark matter. Moreover, the SM has a large number of free parameters that are arbitrarily adjusted, so strongly that it suggests that the SM is not a complete theory and there is an underlying explanation. These are in general "fine-tuning" issues.

One of the most worrying fine-tuning problems of the SM is the "Strong CP problem". It is related to the θ-term of the gauge QCD Lagrangian, which characterizes the QCD vacuum and is CP-odd. That is why it is called strong *CP*-problem. The Lagrangian reads:

$$\mathcal{L}_{QCD} = -\frac{1}{4}G^a_{\mu\nu}G^{a\mu\nu} + i\overline{\psi}\not{D}\psi + \theta\frac{\alpha_s}{8\pi}G^a_{\mu\nu}\tilde{G}^{a\mu\nu} + \left(\overline{\psi}_L M\psi_R + \text{h.c.}\right) , \tag{1.1}$$

where $G^a_{\mu\nu} \equiv \partial_\mu A^a_\nu - \partial_\nu A^a_\mu - g f^a_{bc} A^b_\mu A^c_\nu$ is the gluon field strength tensor, $\tilde{G}^{\mu\nu} \equiv \frac{1}{2}\epsilon^{\mu\nu\rho\sigma}G_{\rho\sigma}$ is the dual field strength tensor and M is the (complex) mass matrix of the fermions that are charged under QCD (quarks), denoted in a compact way by the field $\psi(x)$. It is possible to perform an axial rotation ($U(1)_A$) of the fermion field in such a way that the complex phases of M are *absorbed* into the θ parameter. This results in a new parameter $\overline{\theta}$ that characterizes the CP-odd effects given by:

$$\overline{\theta} = \theta + \text{Arg}\left[\det M\right] . \tag{1.2}$$

This parameter $\overline{\theta}$ is the only one that has a real physical sense, since it is the unique that can be experimentally measured. However, the experimental limits on the neutron electric dipole moment (nEDM) have set an extreme constraint on this parameter: $\overline{\theta} \leq 10^{-10}$ [1].

Since the θ-term is CP-odd, one could be tempted to exclude it by imposing CP invariance. On the other hand, the SM already includes CP-violation in the electroweak (EW) sector, specifically in the fermion mass matrix M, contributing to Eq. (1.2). Why do strong interactions seem not to violate CP then? In other words, why does $\overline{\theta}$ seem to be absent from the Lagrangian? In principle $\overline{\theta}$ could take any value, even smaller than 10^{-10}, and there would not be any mathematical inconsistency in the model. However, if we saw a ball perfectly balanced on top of a hill, we would seek for an explanation behind of that situation. This is a "fine tuned" (possible but uncomfortable) situation. It is puzzling why $\overline{\theta}$ is not of order ~ 1, since there is no reason for the two terms in Eq. (1.2) to cancel.

One possibility is to look for a dynamical mechanism that would explain the smallness of $\overline{\theta}$. Dynamical solutions of fine-tuning problems have been very useful in particle physics (for example, the GIM mechanism and the prediction of the charm quark). The first dynamical solution for the Strong CP problem was proposed by Peccei and Quinn in 1977 [2]. They proposed a new $U(1)_A$ global symmetry, called $U(1)_{PQ}$, in the quark sector, under which the quarks would transform axially. This symmetry would be exact at classical (Lagrangian) level, but would be broken explicitly at quantum level via the chiral anomaly, in such a way that the θ-term could be "erased" from the Lagrangian, as detailed later on. $\overline{\theta}$ becomes unphysical.

Moreover, as no trace of a $U(1)_A$ symmetry is seen in the observed spectrum, $U(1)_{PQ}$ would be spontaneously broken. The Goldstone theorem implies that a new massless Goldstone boson (GB) must exist: the axion. Nevertheless, due to the explicit breaking of $U(1)_{PQ}$ at quantum level, the axion would be instead a pseudo-Goldstone boson (pGB), with a small non-zero mass.

The original Peccei-Quinn-Weinberg-Wilczek (PQWW) axion is ruled out, since the scale of the new physics would be of the order of the electroweak symmetry breaking (EWSB) scale, $v \approx 246$ GeV, which is experimentally excluded due to meson decays [3]. Other models, called *invisible axion* models were proposed, where the scale associated to the new physics is much larger, explaining why the axion has not been detected yet, as all axion couplings are inversely proportional to the axion scale f_a.

On the other hand, the interest in the axion goes beyond particle physics. It is an ideal candidate to explain the composition of dark matter (DM) for which we have plenty of astrophysical and cosmological evidence. DM is a hypothetical neutral matter, whose true nature is unknown, and would form approximately 80% of the total matter of the universe. Many ideas have been suggested in particle physics seeking to explain the true composition of DM. One of the main ideas is the WIMP (weakly interacting massive particle): a hypothetical particle with a mass around ~ 100 GeV that would interact with a strength alike to that of EW interactions. WIMPs could be produced thermally via a freeze-out mechanism in the early universe and could explain the DM relic density observed today. Alternatively, axion are also a viable DM candidate. DM axions could be produced by a totally different mechanism called the *misalignment mechanism*. Few years after the Peccei-Quinn mechanism was published, it was realized that if the scale of the axion was of order $f_a \geq 10^{10}$ GeV, it could be produced non-thermally in the early universe as a "condensate" of axions, that could reproduce the correct DM relic density. This versatility of the axion for solving multiple problems in different fields of physics has turned it into major research topic in particle physics literature.

In this work, I focus on the effective Lagrangians that are used to describe the (possible) couplings of the axion to SM particles. In order to solve the Strong CP problem, all axion models have a coupling to gluons as a consequence of $U(1)_{PQ}$ being anomalous, but, depending on the model, it may also couple to photons and EW bosons or fermions. These effective couplings have been experimentally constrained in very different ways. In particular, one of the most constrained ones is the coupling to photons: it is not only constrained by axion detection experiments, but it is also strongly restricted by astrophysical observations. If the coupling to photons were too large, axions would contribute to the loss of energy via emission of axions in stars and supernovae. Thus, the astrophysical events of this kind that we observe sets strong limits on this coupling. For all axion models, the mass of the axion is related to f_a as: $m_a \propto 1/f_a$. Therefore, the constraints on the couplings have been used to set a "window" of the expected mass of the axion for these models: $m_a \leq 10$ meV and $f_a \geq 10^9$ GeV. If the axion explains all DM, then we can consider a preferred lower limit on the mass too: $m_a \geq 10^{-2}$ meV and $f_a \leq 10^{12}$ GeV. The axion detection experiments, that are mainly based on the coupling to photons, have started to take data in the region where the invisible axion is expected to be found with the ADMX experiment [4]. This has triggered an increasing interest on axion physics in the last years.

Furthermore, the results in this work are also valid for axion-like-particles (ALPs). These are pseudo-Goldstone bosons derived from the spontaneous breaking of a global symmetry, as the axion, but they do not intend to solve the Strong CP problem. They will have derivative effective couplings to SM particles, in a similar way as the axion. One example of these new hypothetical particles is the *Majoron*, that was theorized as the Goldstone bosons associated to the global symmetry $B-L$, that, when spontaneously broken, would give Majorana masses to neutrinos.

As we will see later, even if one of the effective couplings for axion or ALPs is not originally present in the effective Lagrangian at tree level, it can be generated at quantum level (by loops) at a higher order. For example, if the coupling to two photons is set to zero in the effective Lagrangian, but a coupling to electrons is allowed there, axions can still interact with two photons via a triangle loop of electrons: the coupling to photons gets a correction that stems from the coupling to electrons. See Fig. 1.

This property can be used to set new important constraints on couplings that are more difficult to detect experimentally. Since the data on photon-axion interactions are much more constrained than the coupling to electrons, it is possible to set from the former an upper bound for the experimental coupling to electrons.

Basically, most bounds that have been set up to date assume that the axion is produced on-shell, or close to its resonance in particle colliders, and only very recent works are starting to consider *non-resonant* searches of the axion [5]. Non-resonant searches take advantage of the derivative nature of the axion couplings, that become stronger at higher energies. Thus,

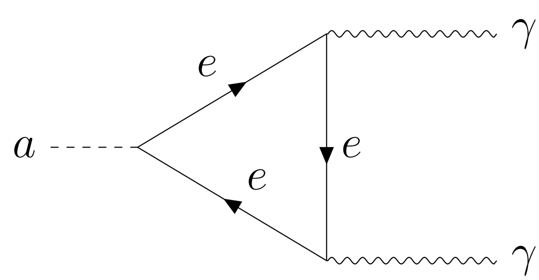

FIG. 1. Axion one-loop induced coupling to two photons through a tree-level effective coupling to electrons.

at typical collider energies, LHC for example, a very light ALP can be produced off-shell and mediate $2 \to 2$ scattering processes in the s channel, such as $gg \to \gamma\gamma$, having a large impact at energies $\sqrt{s} \gg m_a$. Moreover, since this method does not depend on the mass of the axion at such energies, it can be used to exclude large areas in the parameter space for axion couplings.

For this work, we are mainly focusing on the constraints on the axion couplings to fermions that can be set through this novel approach (non-resonant constraints). Better constraints can be derived from the constraints for the coupling with photons, assuming that they are induced by the coupling to fermions. This is the first time this study is done and it constitutes an original contribution.

This work is divided in three sections: in section 2, we explain in depth the basic concepts of the Strong CP problem; in section 3 describes the Peccei-Quinn solutions to the problem, and several axion models are discussed; in section 4 the effective field theories used to describe axion interactions are considered. This latter section also includes the original part of this work. In particular, non-resonant searches are used to put novel constraints on some couplings via its loop-induced effects.

2. STRONG CP PROBLEM

2.1. Instantons in QCD

It can be shown that the last two terms in $\mathcal{L}_{QCD}$ in Eq. (1.1) are odd under a CP transformation. For instance, $G\tilde{G}$ can be rewritten in the classical limit as $-4\vec{E}\cdot\vec{B}$, where $\vec{E}$ and $\vec{B}$ are fields equivalent to the electric and magnetic fields respectively for the strong interactions. This product is odd under P and T, and thus under CP by the CPT theorem. This is in contrast with the term GG, which can be rewritten in the classical limit as $2(B^2 - E^2)$ and is P and CP conserving.

On the other side, the mass matrix M is in general complex. It is always possible to choose a certain basis for the fermion fields at which M is diagonal. Let us denote the eigenstates of M as $m_i e^{i\alpha_i}$, where m_i is a real positive number and α_i is a complex phase. In this basis, we can rewrite the mass term as follows:

$$\begin{aligned}
\left(\overline{\psi}_L M \psi_R + \text{h.c.}\right) &= \sum_i \left(\overline{\psi}_{i,L} m_i e^{i\alpha_i}\psi_{i,R} + \bar{\psi}_{i,R} m_i e^{-i\alpha_i}\psi_{i,L}\right) \,, \\
&= \sum_i m_i \left[(\cos\alpha_i + i\sin\alpha_i)\,\overline{\psi}_{i,L}\psi_{i,R} + (\cos\alpha_i - i\sin\alpha_i)\,\bar{\psi}_{i,R}\psi_{i,L}\right] \,, \\
&= \sum_i m_i \left(\cos\alpha_i \overline{\psi}_i\psi_i + i\sin\alpha_i \overline{\psi}_i\gamma^5\psi_i\right) \,, \\
\alpha_i \ll 1 \Rightarrow \; &\approx \sum_i m_i \left(\overline{\psi}_i\psi_i + i\alpha_i\overline{\psi}_i\gamma^5\psi_i\right) \,.
\end{aligned} \tag{2.1}$$

The first term in the last line in Eq. (2.1) ($\sim \overline{\psi}\psi$) is CP-even. The second term ($\sim \overline{\psi}\gamma^5\psi$) is instead CP-odd. Moreover, the latter is proportional to the complex phases α_i, so, if M is real, the mass term must conserve CP. Later, it will be shown that the mass term and the θ-term are closely related by a $U(1)_A$ transformation of the fermion field $\psi(x)$: the complex phases of the M matrix can be absorbed into the θ parameter, so that all the source of violation of CP is concentrated in a $\sim \overline{\theta}G\tilde{G}$ term.

On the other hand, the θ-term used to be disregarded from the QCD Lagrangian because it is a total derivative. Let us define the vector K^μ:

$$K^\mu \equiv 2\epsilon^{\mu\nu\rho\sigma}A^a_\nu\left(\partial_\rho A^a_\sigma - \frac{2g}{3}f^a_{bc}A^b_\rho A^c_\sigma\right) = \epsilon^{\mu\nu\rho\sigma}A^a_\nu\left(G^a_{\rho\sigma} + \frac{2g}{3}f^a_{bc}A^b_\rho A^c_\sigma\right) \,, \tag{2.2}$$

that satisfies:

$$\partial_\mu K^\mu = \partial_\mu\left[\epsilon^{\mu\nu\rho\sigma}A^a_\nu\left(G^a_{\rho\sigma} + \frac{2g}{3}f^a_{bc}A^b_\rho A^c_\sigma\right)\right] = G^a_{\mu\nu}\tilde{G}^{a\mu\nu} \,, \tag{2.3}$$

where f^a_{bc} are the structure constants of $SU(3)_C$.

This would suggest that the $\sim \overline{\theta} G\tilde{G}$ term does not contribute to the equations of motion (EOM), it only contributes to the action ($S = \int \mathrm{d}^4x\, \mathcal{L}$) as a boundary term, that can be set to zero setting the boundary condition $\lim_{r\to\infty} A^a_\mu \sim \mathcal{O}\left(1/r^{1+\epsilon}\right)$, for $\epsilon > 0$.

However, this is not true. For QCD (and, in general, for non-abelian gauge groups) there are some field configurations that do not decay fast enough at $r \to \infty$, so they add a finite contribution the action S. These configurations are called *instantons* [6] and they are classical solutions of the OEM of the fields in *Euclidean space*. Euclidean spacetime is a reparameterization of Minkovski spacetime, where we define the *Euclidean time* as $\tau \equiv it$, so that the metric turns into Euclidean metric $(+, +, +, +)$. In this space, the Yang-Mills term of the Lagrangian of the gauge interactions is written as:

$$S_E \supset -\frac{1}{2} \int \mathrm{d}^4x \, \mathrm{Tr}\left[G_{\mu\nu}G^{\mu\nu}\right] \, , \tag{2.4}$$

where S_E is the *Euclidean action*, $G_{\mu\nu} \equiv G^a_{\mu\nu} t^a$ and t^a are the generators of the gauge group. In order for this term to have a finite action, we require that, as $r \to \infty$, $G_{\mu\nu}G^{\mu\nu}$ decays faster than r^4 (where $r \equiv (\tau^2 + \vec{x}^2)^{1/2}$):

$$G_{\mu\nu}G^{\mu\nu} \sim \mathcal{O}\left(\frac{1}{r^{4+\epsilon}}\right) \qquad \Rightarrow \qquad G_{\mu\nu} \sim \mathcal{O}\left(\frac{1}{r^{2+\epsilon}}\right) . \tag{2.5}$$

Nevertheless, this does not imply that the field A_μ goes as $\mathcal{O}(1/r^{1+\epsilon})$ at $r \to \infty$. In particular, it can be any gauge transformation of the field $A_\mu = 0$. These configurations are called *pure gauge* configurations. For a field A_μ, the gauge transformed field $A^{(\Omega)}_\mu$ can be computed as:

$$A^{(\Omega)}_\mu = \Omega A_\mu \Omega^{-1} + \frac{i}{g}\Omega\partial_\mu\Omega^{-1} \, , \tag{2.6}$$

where Ω is an element of the gauge group, that we call G. Thus, a pure gauge configuration of A_μ at $r \to \infty$ can be written as:

$$A_\mu = \frac{i}{g}\Omega\partial_\mu\Omega^{-1} + \mathcal{O}\left(\frac{1}{r^{1+\epsilon}}\right) . \tag{2.7}$$

Notice that at $r \to \infty$, $\Omega(x)$ is a function of the 3 angles in the four-dimensional Euclidean space. These solutions are determined by a map from the 3-sphere (at infinity) to the gauge group: $\Omega(x) : S^3 \to G \equiv SU(3)_C$.

It can be shown that for $G \equiv SU(3)_C$ (and in general for $SU(N)$ Lie groups) all these maps can be characterized by an integer ν, that is commonly named *winding number* or *Pontryagin index*. In particular, every map is homotopic to one of the so-called standard maps:

$$\Omega^{(\nu)}(x) = \left(\frac{\tau + i\vec{\sigma}\cdot\vec{x}}{r}\right)^\nu \, , \tag{2.8}$$

where $\vec{\sigma}$ are the Pauli matrices. This means that any map can be continuously deformed into one of the maps described in Eq. (2.8), for some particular ν. However, maps with different ν are not connected through a continuous deformation. In particular, if the vector field A_μ is a configuration with $\nu \neq 0$, it can never be continuously deform to reach the configuration $A_\mu = 0$, that has winding number $\nu = 0$.

Moreover, given the above expressions for Ω, the pure gauge term of A_μ goes as $\mathcal{O}(1/r)$ at $r \to \infty$, so that $G\tilde{G}$ becomes a finite contribution to the action. Using Eq. 2.3 and Gauss theorem, it follows that:

$$\begin{aligned} S_E \supset\propto \int \mathrm{d}^4x\, G^a_{\mu\nu}\tilde{G}^{a\mu\nu} &= \int \mathrm{d}^4x\, \partial_\mu K^\mu\,, \\ &= \int_{r\to\infty} \mathrm{d}^3\sigma_\mu\, K^\mu\,, \\ &= \int_{r\to\infty} \mathrm{d}^3\sigma_\mu\, \epsilon^{\mu\nu\rho\sigma} A^a_\nu \left(G^a_{\rho\sigma} + \frac{2g}{3} f^a_{bc} A^b_\rho A^c_\sigma \right)\,, \end{aligned} \tag{2.9}$$

where $\mathrm{d}^3\sigma_\mu$ is the differential area element in the hypersphere at $r \to \infty$.

As $G^a_{\rho\sigma} \sim \mathcal{O}(1/r^{2+\epsilon})$, the first term in the integral vanishes in the limit $r \to \infty$. Therefore, only the second term remains:

$$\begin{aligned} \int \mathrm{d}^4x\, G^a_{\mu\nu}\tilde{G}^{a\mu\nu} =& \frac{2g}{3} \int_{r\to\infty} \mathrm{d}^3\sigma_\mu\, \epsilon^{\mu\nu\rho\sigma} A^a_\nu A^b_\rho A^c_\sigma f^a_{bc}\,, \\ =& \frac{4g}{3} \int_{r\to\infty} \mathrm{d}^3\sigma_\mu\, \epsilon^{\mu\nu\rho\sigma}\, \mathrm{Tr}\left[A_\nu A_\rho A_\sigma\right]\,, \\ =& -\frac{4i}{3g^2} \int_{r\to\infty} \mathrm{d}^3\sigma_\mu\, \epsilon^{\mu\nu\rho\sigma}\, \mathrm{Tr}\left[\Omega\partial_\nu\Omega^{-1}\Omega\partial_\rho\Omega^{-1}\Omega\partial_\sigma\Omega^{-1}\right]\,, \end{aligned} \tag{2.10}$$

Finally, using the expression of Eq. 2.8 for the maps Ω, it follows that:

$$\int \mathrm{d}^4x\, G^a_{\mu\nu}\tilde{G}^{a\mu\nu} = \frac{32\pi^2\nu}{g^2} = \frac{8\pi\nu}{\alpha_s}\,, \tag{2.11}$$

where $\alpha_s \equiv g^2/4\pi$.

In resume, even though it is a total derivative, the θ-term gives a finite non-zero contribution to the action, that is proportional to the winding number and can have a physical impact. Thus, since this term is a source of violation of CP, we expect QCD to violate this symmetry a priori.

2.2. The ABJ anomaly

In this section I show the explicit relation between the two CP-violating terms of the Lagrangian of QCD. As discussed above, those terms are related by a $U(1)_A$ transformation of the quark fields. In order to show this relation, let us consider a simpler version of the QCD Lagrangian with just one massive quark specie $q(x)$:

$$\mathcal{L} = -\frac{1}{4}G^a_{\mu\nu}G^{a\mu\nu} + \theta\frac{\alpha_s}{8\pi}G^a_{\mu\nu}\tilde{G}^{a\mu\nu} + i\overline{q}\not{D}q - \left(\overline{q}_L m e^{i\alpha} q_R + \text{h.c.}\right) , \tag{2.12}$$

where D_μ is the covariant derivative, m is the mass of the fermion and α is a complex phase. Again, in the approximation $\alpha \ll 1$ (Eq. 2.1) the Lagrangian can be rewritten as:

$$\mathcal{L} = -\frac{1}{4}G^a_{\mu\nu}G^{a\mu\nu} + \theta\frac{\alpha_s}{8\pi}G^a_{\mu\nu}\tilde{G}^{a\mu\nu} + \overline{q}\left(i\not{D} - m\right)q - i\alpha m\overline{q}\gamma^5 q\,. \tag{2.13}$$

A $U(1)_A$ can be implemented such that:

$$q \to e^{i\beta\gamma^5}q = \begin{cases} e^{+i\beta}q_R \\ e^{-i\beta}q_L \end{cases} \qquad \overline{q} \to \overline{q}e^{i\beta\gamma^5} = \begin{cases} e^{-i\beta}\overline{q_R} \\ e^{+i\beta}\overline{q_L} \end{cases} \tag{2.14}$$

This transformation relates the two sources of violation of CP that can be present in the QCD Lagrangian. Now the question is: how exactly are these terms related? In order to answer this question first we have to check how the mass term transforms under $U(1)_A$:

$$-i\alpha m\overline{q}\gamma^5 q \xrightarrow{U(1)_A} -i(\alpha + 2\beta)m\overline{q}\gamma^5 q\,. \tag{2.15}$$

This makes explicit that the chiral transformation shifts the complex phase in the mass matrix of the fermions. The constant β is arbitrary, and by choosing $\beta = -\alpha/2$ the phase in the mass matrix is eliminated.

As it was shown, the *chiral current* (j^μ_5) associated to the axial transformation $U(1)_A$ is not conserved at classical level. In other words, at classical level the Lagrangian is not invariant under this transformation due to the mass term of the fermions:

$$\partial_\mu j^\mu_5 = \frac{\delta\mathcal{L}}{\beta} = -i2m\overline{q}\gamma^5 q\,. \tag{2.16}$$

However, this is not the end of the story. The current j^μ_5 is broken explicitly by another term at quantum level. This means that is induced by loop diagrams. This term is called the chiral anomaly or ABJ anomaly (because of the name of its discoverers Adler-Bell-Jackiw), and can be calculated by different methods, such as dimensional regularization or the Fujikawa method. In this work I am following the derivation presented in Ref. [7]. First, the chiral anomaly is computed in the electromagnetic sector (QED), since the extension to QCD form QED is trivial. In order to do this, it is necessary to check that the divergence of the chiral current has a non-zero matrix element for two photons creation:

$$\int \mathrm{d}^4x\, e^{-ipx}\, \langle q_1, q_2|\, \partial_\lambda j^\lambda_5\, |0\rangle = (2\pi)^4\delta(q_1 + q_2 - p)\varepsilon^*_\mu(q_1)\varepsilon^*_\nu(q_2) i p_\lambda \mathcal{M}^{\lambda\mu\nu}\,, \tag{2.17}$$

where ε^*_μ is the polarization vector of one of the photons, q_1 and q_2 are the momenta of the photons and $p\,(= q_1 + q_2)$ is the momentum associated to the chiral current. $\mathcal{M} \equiv ip_\lambda \varepsilon^*_\mu(q_1)\varepsilon^*_\nu(q_2)\mathcal{M}^{\lambda\mu\nu}$ is Feynman amplitude of the process.

The leading-order diagrams that contribute to $\mathcal{M}^{\lambda\mu\nu}$ are those in Fig. (2):

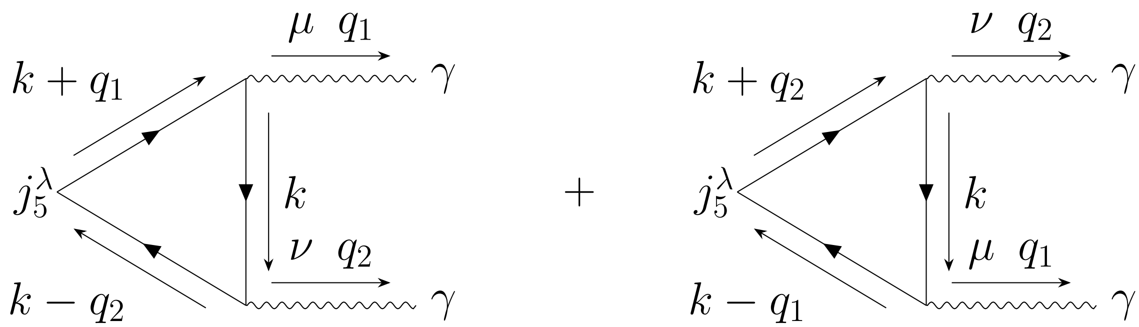

FIG. 2. Triangle loop diagrams that break the chiral current j_5^μ at quantum level, where the fermions ψ run in the loop.

Let us consider first only the diagram in Fig. 2 left. Neglecting the fermion masses, the contribution of this diagram to the amplitude is given by:

$$\mathcal{M}^{\lambda\mu\nu} = (-1)(ieQ_\psi)^2 \int \frac{\mathrm{d}^4k}{(2\pi)^4} \,\mathrm{Tr}\left[\gamma^\lambda\gamma^5 \frac{i(\not{k} - \not{q}_2)}{(k - q_2)^2}\gamma^\nu \frac{i\not{k}}{k^2}\gamma^\mu \frac{i(\not{k} + \not{q}_1)}{(k + q_1)^2}\right], \tag{2.18}$$

where Q_ψ is the electric charge of the fermions in the loop. Notice also that the chiral current enters in the amplitude as a factor $\gamma^\lambda\gamma^5$. Taking the divergence of the chiral current in Eq. (2.17) is equivalent to contracting this expression with the momentum ip_λ associated to the current: $\partial_\lambda j_5^\lambda \to ip_\lambda j_5^\lambda$. Thus:

$$ip_\lambda\mathcal{M}^{\lambda\mu\nu} = e^2Q_\psi^2 \int \frac{\mathrm{d}^4k}{(2\pi)^4} \,\mathrm{Tr}\left[\not{p}\gamma^5 \frac{(\not{k} - \not{q}_2)}{(k - q_2)^2}\gamma^\nu \frac{\not{k}}{k^2}\gamma^\mu \frac{(\not{k} + \not{q}_1)}{(k + q_1)^2}\right]. \tag{2.19}$$

Furthermore, as $p = q_1 + q_2$, $\not{p}\gamma^5$ can be rewritten as follows:

$$\not{p}\gamma^5 = (\not{k} + \not{q}_1)\gamma^5 + \gamma^5(\not{k} - \not{q}_2)\,, \tag{2.20}$$

and in consequence:

$$ip_\lambda\mathcal{M}^{\lambda\mu\nu} = e^2Q_\psi^2 \int \frac{\mathrm{d}^4k}{(2\pi)^4} \,\mathrm{Tr}\left[\gamma^5 \frac{(\not{k} - \not{q}_2)}{(k - q_2)^2}\gamma^\nu \frac{\not{k}}{k^2}\gamma^\mu - \gamma^5 \frac{\not{k}}{k^2}\gamma^\mu \frac{(\not{k} + \not{q}_1)}{(k + q_1)^2}\gamma^\nu\right]. \tag{2.21}$$

Naively, it would seem that if we now shift k in the first term of this expression by $k \to k + q_2$ we obtain a quantity that is manifestly antisymmetric under $q_1 \leftrightarrow q_2$ and $\mu \leftrightarrow \nu$.

The second diagram gives precisely the same contribution but with q_1 and q_2, and μ and ν interchanged. So that, it cancels exactly with the former.

The integral that we are shifting is linearly divergent, though. So that, the shift in k is not allowed before using a regularization method. One way to deal with these divergences is to compute the integrals using dimensional regularization, because it ensures the validity of the QED Ward identities. On the other hand, γ^5 is intrinsically a four-dimensional object and it has to be treated with care. One way to proceed is to keep the definition of γ^5 in four dimensions: $\gamma^5 = i\gamma^0\gamma^1\gamma^2\gamma^3$, which anticommutes with γ^μ for $\mu \leq 3$, but commutes for $\mu > 3$. The momenta p, q_1 and q_2 are in the physical dimensions, but the momentum k that is running in the loop has non-zero components in all dimensions. Let us define:

$$k \equiv k_\parallel + k_\perp \,, \tag{2.22}$$

where $k_\parallel$ only has non-zero components in the physical dimensions (so it anticommutes with γ^5) and $k_\perp$ only has non-zero components in the other $d-4$ dimensions (it commutes). Going back to Eq. (2.19) and substituting:

$$\not{p}\gamma^5 = (\not{k} + \not{q}_1)\gamma^5 + \gamma^5(\not{k} - \not{q}_2) - 2\gamma^5\not{k}_\perp \,. \tag{2.23}$$

The contribution of the first two terms of this expression vanish because of the same reasons that we gave for Eq. (2.21). Now dimensional regularization is being considered and the integration variable k can be safely shifted. Nevertheless, we are left with an extra term that contributes to the amplitude as follows:

$$ip_\lambda \mathcal{M}^{\lambda\mu\nu} = -2e^2Q_\psi^2 \int \frac{\mathrm{d}^dk}{(2\pi)^d} \operatorname{Tr}\left[\gamma^5\not{k}_\perp \frac{(\not{k} - \not{q}_2)}{(k-q_2)^2}\gamma^\nu \frac{\not{k}}{k^2}\gamma^\mu \frac{(\not{k} + \not{q}_1)}{(k+q_1)^2}\right] . \tag{2.24}$$

The Feynman parameterization of the integrand in convenient:

$$\frac{1}{k^2(k-q_2)^2(k+q_1)^2} = \int_0^1 \mathrm{d}x \int_0^{1-x} \mathrm{d}y \, \frac{2}{\left[k^2 + xq_1^2 + yq_2^2 + 2k(xq_1 - yq_2)\right]^3} \,. \tag{2.25}$$

The integration variable k can be shifted as $k \to k - xq_1 + yq_2$. Therefore, the denominator can be rewritten as: $[k^2 - \Delta]^3$, where:

$$\Delta \equiv -x(1-x)q_1^2 - y(1-y)q_2^2 - 2xyq_1q_2 \,. \tag{2.26}$$

On the other hand, when the numerator is expanded only one factor of each γ^μ, γ^ν, $\not{q}_1$ and $\not{q}_2$ has to be retained to give a non-zero trace with γ^5. The remaining factors $\not{k}$ and $\not{k}_\perp$

can be moved to adjacent positions, since $\not{k}_\perp$ anticommutes with the other gamma matrices in the problem. Applying then:

$$\not{k}\not{k}_\perp = \not{k}_\perp\not{k}_\perp = (k_\perp)^2 \,, \tag{2.27}$$

the numerator is written as:

$$\mathrm{Tr}\left[\gamma^5\not{k}_\perp(\not{k}-\not{q}_2)\gamma^\nu\not{k}\gamma^\mu(\not{k}+\not{q}_1)\right] = -k_\perp^2\,\mathrm{Tr}\left[\gamma^\mu\gamma^\nu\not{q}_1\not{q}_2\gamma^5\right] = i4\epsilon^{\mu\nu\alpha\beta}q_{1\alpha}q_{2\beta}k_\perp^2 \,. \tag{2.28}$$

Notice that this expression is invariant under the shift in the integration momentum, so the total amplitude of the diagram can be written as follows:

$$ip_\lambda\mathcal{M}^{\lambda\mu\nu} = -i16e^2Q_\psi^2\epsilon^{\mu\nu\alpha\beta}q_{1\alpha}q_{2\beta}\int_0^1\mathrm{d}x\int_0^{1-x}\mathrm{d}y\int\frac{\mathrm{d}^dk}{(2\pi)^d}\frac{k_\perp^2}{[k^2-\Delta]^3}\,. \tag{2.29}$$

The momentum integral can be solved in spherical coordinates:

$$\int\frac{\mathrm{d}^dk}{(2\pi)^d}\frac{k_\perp^2}{[k^2-\Delta]^3} = \frac{(d-4)}{d}\int\frac{\mathrm{d}^dk}{(2\pi)^d}\frac{k^2}{[k^2-\Delta]^3} = \frac{i(d-4)}{2(4\pi)^{d/2}}\frac{\Gamma(2-d/2)}{\Gamma(3)\Delta^{2-d/2}} \overset{d\to4}{=} \frac{-i}{2(4\pi)^2}\,. \tag{2.30}$$

This result does not depend on the Feynman parameters, x and y.

In summary,

$$ip_\lambda\mathcal{M}^{\lambda\mu\nu} = -\frac{e^2Q_\psi^2}{4\pi^2}\epsilon^{\mu\nu\alpha\beta}q_{1\alpha}q_{2\beta}\,. \tag{2.31}$$

This term is symmetric under the interchange $q_1 \leftrightarrow q_2$ and $\mu \leftrightarrow \nu$, so the second diagram only adds a factor 2 in the coefficient. Finally, the following expression for the divergence of the chiral current is obtained:

$$\begin{aligned}\langle q_1,q_2|\,\partial_\lambda j_5^\lambda\,|0\rangle =& \frac{e^2Q_\psi^2}{2\pi^2}\epsilon^{\mu\nu\alpha\beta}\left(-iq_{1\alpha}\right)\varepsilon_\mu^*(q_1)\left(-iq_{2\beta}\right)\varepsilon_\nu^*(q_2)\,,\\ =& -\frac{e^2Q_\psi^2}{16\pi^2}\langle q_1,q_2|\,\epsilon^{\alpha\mu\beta\nu}F_{\alpha\mu}F_{\beta\nu}\,|0\rangle\;.\end{aligned} \tag{2.32}$$

and in consequence:

$$\partial_\mu j_5^\mu = -\frac{e^2Q_\psi^2}{8\pi^2}F_{\mu\nu}\tilde{F}^{\mu\nu} = -Q_\psi^2\frac{\alpha_{em}}{2\pi}F_{\mu\nu}\tilde{F}^{\mu\nu}\,, \tag{2.33}$$

where $\alpha_{em} = e^2/4\pi$ is the fine-structure constant of QED. This is the axial anomaly in the QED sector.

The contribution of the QCD anomaly can be obtained by replacing: $F\tilde{F} \to G^a\tilde{G}^b$, $\alpha_{em} \to \alpha_s$ and $Q_\psi^2 \to \mathrm{Tr}\left[t^at^b\right] = \delta^{ab}/2$, where $\alpha_s \equiv g^2/4\pi$ is the strong coupling constant and t_a are the generators of $SU(3)_C$. The QCD anomaly is given by the next expression:

$$\partial_\mu j_5^\mu = -\frac{\alpha_S}{4\pi}G_{\mu\nu}^a\tilde{G}^{a\mu\nu}\,. \tag{2.34}$$

Finally, we can put together this result with the explicit violation of the chiral current at classical level, induced by the mass term of the fermions, that we computed before:

$$\partial_\mu j_5^\mu = -i2m\bar{q}\gamma^5 q - \frac{\alpha_S}{4\pi}G^a_{\mu\nu}\tilde{G}^{a\mu\nu}\,. \tag{2.35}$$

It is clear that the result in Eq. (2.15) was incomplete. When we make a transformation $U(1)_A$ of angle β, the Lagrangian is modified as: $\delta\mathcal{L} = \beta\partial_\mu j_5^\mu$. As a consequence, by choosing $\beta = -\alpha/2$, we can "erase" the complex phase in the mass of the fermions and absorb it into the θ-term:

$$\mathcal{L} \xrightarrow{U(1)_A,\,\beta=-\alpha/2} \mathcal{L}' = -\frac{1}{4}G^a_{\mu\nu}G^{a\mu\nu} + \bar{\theta}\frac{\alpha_s}{8\pi}G^a_{\mu\nu}\tilde{G}^{a\mu\nu} + \bar{q}\left(i\not{D} - m\right)q\,, \tag{2.36}$$

where $\bar{\theta} \equiv \theta + \alpha$ is the combination of the original theta term and the phase of the masses. It is the only parameter that has a true physical meaning, the only one that can be measured.

Moreover, when we consider several fermions with colour charge, as in Eq. (2.1), we can remove all the phases in the mass matrix M by making a $U(1)_A$ for every fermion, each of them with an angle $\beta_i = -\alpha_i/2$. Thus, at the end the $\bar{\theta}$ parameter that we obtain is:

$$\bar{\theta} = \theta + \mathrm{Arg}\left[\det M\right]\,, \tag{2.37}$$

where $\mathrm{Arg}[\det M] = \sum_i \alpha_i$.

2.3. Neutron electric dipole moment

Experimentally, the most sensitive probe of $\bar{\theta}$ parameter is the data on the electric dipole moment of the neutron (nEDM). This quantity is strongly suppressed in the SM, and thus it is one of the best windows to look for new physics BSM. At Lagrangian level, the nEDM coupling to a given quark q reads:

$$\mathcal{L}^{EDM} = -\frac{i}{2}d_q\bar{q}\sigma_{\mu\nu}\gamma^5 qF^{\mu\nu} \supset -id_q\bar{q}\left(\vec{\sigma}\cdot\vec{E}\right)q\,, \tag{2.38}$$

where d_q is the quark electric dipole moment and $\vec{E}$ the electric field and $\vec{\sigma}$ denotes the fermion spin.

This term in Eq. (2.38) is a coupling with a mass dimension 5 operator and in consequence not present in the SM Lagrangian. It is induced at multi-loop level.

Unlike the magnetic moment, $\mathcal{L}^{MDM} \supset\sim \mu_q\bar{q}\sigma_{\mu\nu}qF^{\mu\nu} \sim \mu_q\bar{q}\left(\vec{\sigma}\cdot\vec{B}\right)q$ (with μ_q the quark dipole moment and $\vec{B}$ the magnetic field), the electric dipole moment changes its direction under P and T (and thus under CP), so that, in order to produce a finite EDM, we require a P and CP-odd coupling to intervene.

Since CP is violated in the SM, it is convenient to ask, if $\overline{\theta} = 0$, what contribution is generated by the weak interactions. Putting aside the complex phase of the PMNS matrix for neutrino mixing, the only source of violation of CP is the complex phase of the CKM (Cabibbo–Kobayashi–Maskawa) matrix [8]. However, CP violation in the SM requires the simultaneous presence of 3-families and non-vanishing mixings. The process is then not possible at one-loop order. Technically, at one-loop level the CKM matrix V_{ij} in the two vertices involving the W boson cancels its phase. The simplest hypothetical one-loop contribution to nEDM (in terms of the valence quarks of the neutron) would be given by the following diagram (Fig. 3):

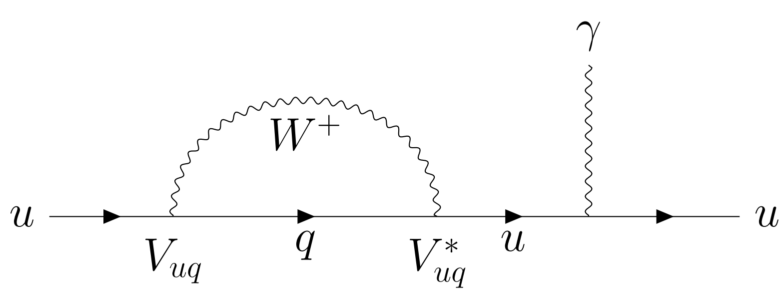

FIG. 3. One-loop hypothetical contribution to nEDM in the SM.

The amplitude of this diagram goes as:

$$\mathcal{M} \sim V_{uq} V^*_{uq} = 1\,, \tag{2.39}$$

Therefore, the next step is to look for a contribution to the quarks EDM in a two-loop diagram [9]. See for example Fig. 4 for one of the diagrams contributing:

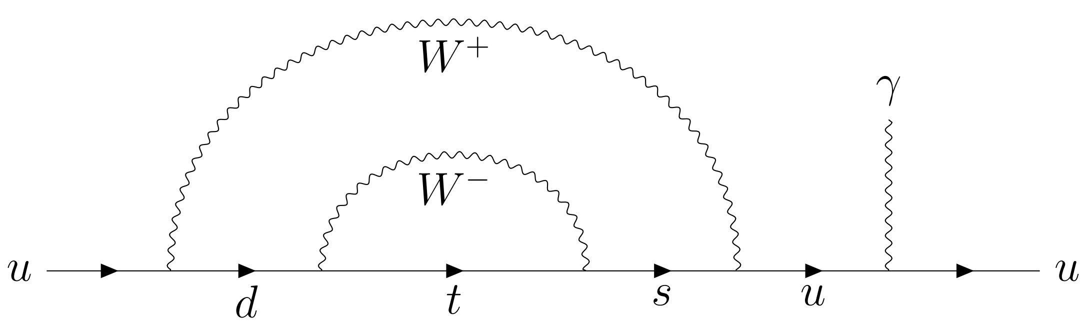

FIG. 4. Two-loop contribution to nEDM in the SM.

For each two-loop diagram alike to that in Fig. 4, the dependence of the amplitude on the CKM matrix elements behaves as:

$$\mathcal{M} \sim V_{uq} V^*_{qq'} V_{q''q'} V^*_{uq'} \,, \tag{2.40}$$

However, it was shown in Ref. [10] that the sum of all two-loop contributions vanishes. As a consequence, in the SM the leading order contribution to the nEDM is given by the three-loop processes such as that in Fig. 5:

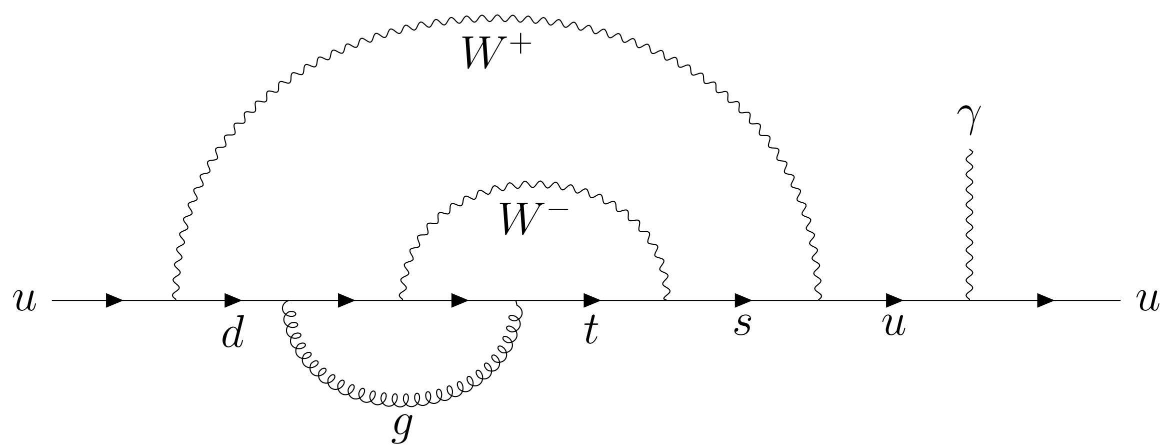

FIG. 5. Leading order contribution to nEDM in the SM.

When we consider the neutron and not only singular quarks, other diagrams at the same EW and QCD level are possible [11, 12]. For example, the diagram shown in Fig. 6.

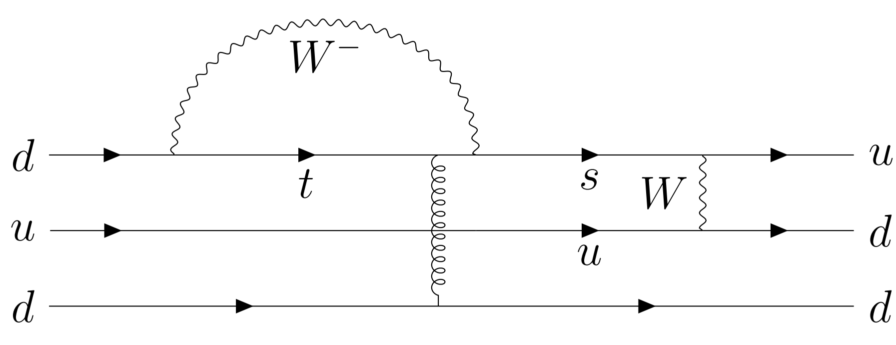

FIG. 6. Valence quarks contribution to nEDM in the SM.

Overall, in the SM nEDM induced by EW interactions is expected to be of order [13, 14]:

$$d_n^{SM} \sim 10^{-31} \;\; \mathrm{e} \cdot \mathrm{cm} \tag{2.41}$$

On the other hand, the θ-term can give by itself an extra contribution to the nEDM beyond SM. In particular, as discussed in the previous section, a $U(1)_A$ transformation of the fermion field can trade the θ-term by a term $i\overline{\theta}m\bar{q}\gamma^5 q \subset \mathcal{L}$. This term gives a finite contribution to the nEDM via the diagram in Fig. 7.

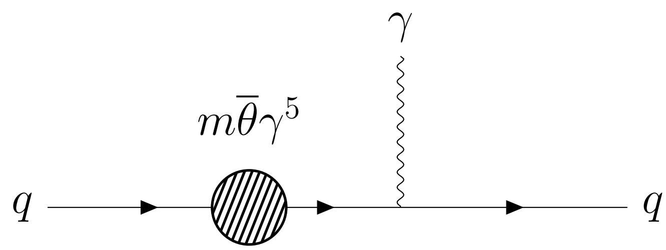

FIG. 7. Feynman diagram of the contribution of the θ-term to the nEDM.

Estimates of the nEDM based on this coupling [15] claim a value for d_n of order:

$$d_n \sim 10^{-16}\overline{\theta} \ \text{e} \cdot \text{cm} \,. \tag{2.42}$$

According to Particle Data Group 2018 data [16]: $d_n^{exp} < 3.0 \cdot 10^{-26}$ e·cm. Then, this translates into the following constraint for the $\overline{\theta}$ parameter:

$$\overline{\theta} < 10^{-10} \,, \tag{2.43}$$

which is puzzling as in the SM the value of $\overline{\theta}$ is not protected by any symmetry.

Future prospects on hadron EDMs for the nEDM are to reach an experimental sensitivity of 10^{-30} e·cm. Also, proton EDM in coming into play with the same expected sensitivity, using storage rings. These projects are gathered in the European Strategy for Particle Physics Update 2018-2020 [17].

3. PECCEI-QUINN SOLUTIONS TO THE STRONG CP PROBLEM: THE AXION

3.1. Massless fermions with colour charge

One of the simplest ways to solve the Strong CP problem arises when we consider the possibility of having massless fermions that are charged under QCD. The Lagrangian for such fermions would be given by:

$$\mathcal{L} = -\frac{1}{4} G^a_{\mu\nu} G^{a\mu\nu} + \overline{\theta} \frac{\alpha_s}{8\pi} G^a_{\mu\nu} \tilde{G}^{a\mu\nu} + i\overline{q} \not{D} q \,. \tag{3.1}$$

As indicated in Eq. (2.35), the divergence of the chiral current would be, in this case, broken only by the chiral anomaly.

A $U(1)_A$ rotation of the massless fermions by an angle $\beta = \overline{\theta}/2$ shows that the θ-term can be reabsorbed away, and the Lagrangian reduces to:

$$\mathcal{L} = -\frac{1}{4} G^a_{\mu\nu} G^{a\mu\nu} + i\overline{q} \not{D} q \,. \tag{3.2}$$

That is, $\overline{\theta}$ has become unphysical and there would be no Strong CP problem! Unfortunately, all the known quarks of the SM seem to be massive. One possibility could be the lightest quark in the SM, the up-quark, to be massless, but this idea is strongly disfavored by lattice QCD simulations [18]. Nevertheless, the case of an hypothetical massless quark suggest how to solve it: to require a new global $U(1)_A$ symmetry that is conserved at classical level but explicitly broken at quantum level by the axial anomaly. Is it possible to enlarge the SM by such a symmetry, but keeping the known quarks massive?

The answer to this question is yes, as proposed by Roberto D. Peccei and Helen R. Quinn [2]. Briefly, Peccei-Quinn solutions impose a new global symmetry under which the fermions transforms axially (usually called $U(1)_{PQ}$) that is conserved at classical level and broken at quantum level (as required). In addition, it is also spontaneously broken.

In the following sections I review the original PQWW axion (that is experimentally ruled out at present), as well as other alternative axion models that are still being considered: invisible axion and heavy axion models.

3.2. Peccei-Quinn-Weinberg-Wilczek axion

In the SM, the mechanism that is responsible for the mass of the fermions is the Higgs mechanism. In particular, the quarks gain their masses due to the Yukawa couplings with the Higgs doublet, when the Higgs field takes a non-zero vacuum expectation value (vev). Let us consider only the Yukawa couplings for the up-quark and the down-quark:

$$\mathcal{L} \supset -Y_d \overline{q}_L \Phi d_R - Y_u \overline{q}_L \tilde{\Phi} u_R + \text{h.c.}\,, \tag{3.3}$$

where Y_q is the Yukawa coupling of the quarks. u_R and d_R are the right-handed quark fields singlets of $SU(2)_L$, q_L is the left-handed quark doublet and Φ is the Higgs doublet. $\tilde{\Phi}$ is defined as $\tilde{\Phi} = i\sigma_2 \Phi^*$.

Let us consider only the first term and try to implement a new symmetry $U(1)_{PQ}$ on it. The fermion fields have to transform axially: $u_R(d_R) \to e^{i\beta} u_R(d_R)$ and $q_L \to e^{-i\beta} q_L$. The Φ Higgs doublet can transform under $U(1)_{PQ}$, as $\Phi \to e^{-i2\beta}\Phi$, and indeed the up quark mass term by itself would be $U(1)_{PQ}$ invariant. However, the second term in Eq. (3.5) goes with $\tilde{\Phi} = i\sigma_2\Phi^*$, which necessarily transforms with the opposite phase: $\tilde{\Phi} \to e^{i2\beta}\tilde{\Phi}$. Therefore, we cannot make both terms classically invariant under $U(1)_{PQ}$ simultaneously: given the Yukawa couplings of the SM for the quarks, it does not exhibit the necessary classically exact $U(1)_A$ global symmetry.

R. Peccei and H. Quinn [2] overcame this situation introducing one extra Higgs doublet to the SM: Φ_1 and Φ_2. Now it is possible $\Phi_1 \to e^{-i2\beta}\Phi_1$ and $\tilde{\Phi}_2 \to e^{-i2\beta}\tilde{\Phi}_2$ under $U(1)_{PQ}$ Considering only the up-quark and the down-quark, the QCD Lagrangian of this model can be written as:

$$\mathcal{L} = -\frac{1}{4} G^a_{\mu\nu} G^{a\mu\nu} + \overline{\theta}\frac{\alpha_s}{8\pi} G^a_{\mu\nu}\tilde{G}^{a\mu\nu} + i\sum_{u,d} \overline{q} \not{D} q + \mathcal{L}_Y + \frac{1}{2}\sum_i D_\mu \Phi_i^\dagger D^\mu \Phi_i - V(\Phi_1, \Phi_2)\ , \tag{3.4}$$

where $V(\Phi_1, \Phi_2)$ is the potential of the two Higgs doublets and $\mathcal{L}_Y$ is the new Yukawa Lagrangian:

$$\mathcal{L}_Y = -Y_d \overline{q}_L \Phi_1 d_R - Y_u \overline{q}_L \tilde{\Phi}_2 u_R + \text{h.c.}\,. \tag{3.5}$$

Notice that, since $\mathcal{L}$ has to be gauge invariant, the hypercharges of the two Higgs doublets have to be: $Y(\Phi_1) = Y(\Phi_2) = 1/2$.

Given this Lagrangian, now we define the $U(1)_{PQ}$ transformation as:

$$u_R, d_R \to e^{i\beta} u_R, d_R\,, \qquad q_L \to e^{-i\beta} q_L\,, \qquad \Phi_1 \to e^{-i2\beta}\Phi_1\,, \qquad \Phi_2 \to e^{+i2\beta}\Phi_2\,. \tag{3.6}$$

that is a good symmetry of the Lagrangian at classical level if the potential $V(\Phi_1, \Phi_2)$ is chosen so that it is invariant under the $U(1)_{PQ}$ global symmetry. The $\overline{\theta}$-term can be rotated away, as the symmetry is explicitly broken at quantum level by the axial anomaly.

Now, Φ_1 and Φ_2 must take a non-zero vev to explain the EW scale ($v \approx 246$ GeV) and give masses to all fields. This means that the new symmetry $U(1)_{PQ}$ is spontaneously broken in the PQ theory. The excitations of the Higgses Φ_1 and Φ_2 around their vev's can be parameterized as follows [19, 20]:

$$\Phi_1 = \frac{1}{\sqrt{2}} \exp\left(i\eta_1/v_1\right) \begin{pmatrix} \rho_1^+ \\ v_1 + \rho_1^0 \end{pmatrix}, \qquad \Phi_2 = \frac{1}{\sqrt{2}} \exp\left(i\eta_2/v_2\right) \begin{pmatrix} \rho_2^+ \\ v_2 + \rho_2^0 \end{pmatrix}, \tag{3.7}$$

where v_1 and v_2 are the vev's of the Higgses (not necessarily equal). The EWSB scale is defined in terms of v_1 and v_2 as: $v = \sqrt{v_1^2 + v_2^2}$. The degrees of freedom of the Higgs doublets Φ_1 and Φ_2 are characterized by the bosons fields ρ_1^0, ρ_1^+, ρ_2^0, ρ_2^+: combinations of these fields result, after EWSB, in the Higgs scalar of the SM, the would-be Goldstone bosons that are "eaten" by the $W^\pm$ bosons (in the unitary gauge, to gain mass) and extra Higgs fields that appear in this model. η_1 and η_2 are the Goldstone bosons associated to two different $U(1)_1$ and $U(1)_2$ symmetries that consist on rotating independently each of both Higgses with a different complex phase:

$$U(1)_1 : \Phi_1 \to e^{i\beta_1/2}\Phi_1\,, \qquad U(1)_2 : \Phi_2 \to e^{i\beta_2/2}\Phi_2\,. \tag{3.8}$$

Notice that $U(1)_{PQ}$, in the Higgs sector, is just a combination of these two symmetries in which they both rotate with the opposite phase: $\beta_1 = -\beta_2 = -4\beta$. The Goldstone boson associated to $U(1)_{PQ}$ is the axion, as expected. However, there is another combination of $U(1)_1$ and $U(1)_2$, orthogonal to $U(1)_{PQ}$, in which both Higgses rotate with the same phase ($\beta_1 = \beta_2$). This is the hypercharge gauge symmetry of the SM $U(1)_Y$: $U(1)_1 \times U(1)_2 = U(1)_{PQ} \times U(1)_Y$.

The Goldstone boson associated to $U(1)_Y$, denoted by G, is the would-be Goldstone boson that is "eaten" by the Z boson in order to gain mass in the unitary gauge. Both GBs (G and the axion a) are related to η_1 and η_2 by the following rotation:

$$\begin{pmatrix} G \\ a \end{pmatrix} = \begin{pmatrix} \cos\delta & \sin\delta \\ -\sin\delta & \cos\delta \end{pmatrix} \begin{pmatrix} \eta_2 \\ \eta_1 \end{pmatrix}, \tag{3.9}$$

where δ is defined as: $\tan\delta \equiv v_1/v_2$.

However, the scale associated to the axion physics f_a in this model would be of order $f_a \approx v = 246$ GeV, as required by the W boson mass in order to satisfy $M_W = gv/2$. The axion has not been observed in experiments yet, and an axion scale f_a of the order of the scale of the EW symmetry breaking is ruled out, for example, by the data on meson decays [3] among others. Therefore, the simplest PQ axion model is currently ruled out, and more sophisticated models are needed in order to solve the Strong CP problem.

Also, we have to highlight that, since $U(1)_{PQ}$ is explicitly broken by the chiral anomaly, the axion is not an exact Goldstone boson. Instead, it is a pseudo-Goldstone boson (pGB), so it has a small but non-zero mass. In particular, it can be shown that the mass of the axion is given by the following expression [22]:

$$m_a f_a \approx m_\pi f_\pi \frac{\sqrt{m_u m_d}}{m_u + m_d}\,, \tag{3.10}$$

where m_u, m_d and m_π are the masses of the up-quark, down-quark and the pion respectively, and f_π is the *pion decay constant* ~ 130 MeV. Moreover, this equation also holds for the invisible axion models, that we present in the next section.

Thus, according to Eq. (3.10), the PQWW axion would have had a mass of order $m_a \sim 10$ keV.

3.3. Invisible axion models

There is a way to save the Peccei-Quinn type of solutions to the Strong CP problem, which consists on introducing a new scale $f_a \gg v$ for the axion physics. The point is that all axion couplings to SM fields are proportional to $1/f_a$, and thus for very large f_a values the experimental constraints on the scale are respected. These models are called *invisible axion models*. In this section I present the two most relevant invisible axion models: the DFSZ axion and the KSVZ axion. Both models raise the scale via the addition of an extra scalar singlet under the SM gauge group, but carrying PQ charges, whose vev $\sim f_a \gg v$.

3.3.1. DFSZ axion

The DFSZ axion model [23, 24], can be understood as an extension of the PQ axion. This model also introduces a second Higgs doublet Φ_2, but it also requires a new complex scalar S. This scalar would be a singlet of the SM gauge group $SU(3) \times SU(2) \times U(1)$, but it would be charged under $U(1)_{PQ}$. In particular, they transform under this symmetry as:

$$\Phi_1 \to e^{-i2\beta}\Phi_1\,, \qquad \Phi_2 \to e^{-i2\beta}\Phi_2\,, \qquad S \to e^{i4\beta} S\,. \tag{3.11}$$

The Yukawa Lagrangian is the same as before: the mass of the fermions are still generated by the non-zero vev's of the two Higgses. However, the potential of the Higgses and the new scalar, $V(\Phi_1, \Phi_2, S)$ introduces couplings between the Higgs doublets and S, for example

$\sim \Phi_1 \tilde{\Phi}_2 S$, and is now defined in such a way that S also takes a non-zero vev, that satisfies:

$$\langle S \rangle = \frac{v_S}{\sqrt{2}} \gg v = \sqrt{v_1^2 + v_2^2} \,. \tag{3.12}$$

Then, we can parameterize the new scalar as follows:

$$S = \frac{1}{\sqrt{2}}(v_s + \rho) e^{i\eta_s / v_s} \,, \tag{3.13}$$

where ρ is the massive excitations field and η_s is the field that characterizes the axial excitations of S.

The DFSZ axion (a) appears in this model as a linear combination of the former PQWW axion and η_s. Given the transformation laws of Φ_1, Φ_2 and S under $U(1)_{PQ}$ of Eq. (3.11), it can be found that a is shifted under this rotation as follows:

$$a \xrightarrow{U(1)_{PQ}} a + \alpha \sqrt{v^2 + \left(\frac{v_s}{2}\right)^2} \,, \tag{3.14}$$

Then, the scale of the axion physics reads:

$$f_a = \sqrt{v^2 + \left(\frac{v_s}{2}\right)^2} \overset{v_s \gg v}{\approx} \frac{v_s}{2} \gg v \,. \tag{3.15}$$

For large v_s, the DFSZ axion has in consequence a much larger scale f_a. Therefore, its couplings to SM particles are very suppressed. Also, because of Eq. (3.10), the axion is much lighter than that of the original PQ model.

3.3.2. KSVZ axion

The KSVZ axion [25, 26] model has the advantage that the Lagrangian of the SM remains intact, and all the new physics is reserved for a new sector made of an extra quark Q, that has at least colour charge, and a new complex scalar S that is a singlet of the whole gauge group of the SM. Likewise, there is a new $U(1)_{PQ}$ symmetry in this sector that rotates the particles as:

$$Q_R \to e^{i\beta} Q_R \,, \qquad Q_L \to e^{-i\beta} Q_L \,, \qquad S \to e^{-i2\beta} S \,. \tag{3.16}$$

Notice that Q transforms axially under this rotation, so, as Q is charged under $SU(3)_C$, this symmetry is broken at quantum level by the chiral anomaly. Therefore, the Strong CP problem is solved. Additionally, the SM particles do not rotate under $U(1)_{PQ}$.

The Lagrangian of the exotic sector is given by the following expression:

$$\mathcal{L} \supset \mathcal{L}_{PQ} = i\overline{Q} \not{D} Q - \left(S \overline{Q}_L Q_R + \text{h.c.} \right) + \frac{1}{2} \partial_\mu S^* \partial^\mu S - V(S) \,, \tag{3.17}$$

where $V(S) = \mu^2|S|^2/2 + \lambda|S|^4/4$, and μ and λ are some constants. If $\mu^2 < 0$, the scalar field S takes a non-zero vev, that in this model corresponds to the scale of the axion physics, that is assumed to be much larger than the scale of the EWSB:

$$\mu^2 < 0 \Rightarrow \langle S \rangle = \sqrt{\frac{-\mu^2}{\lambda}} \equiv f_a \gg v\,. \tag{3.18}$$

Thus, S can be parameterize as: $S = (f_a + \rho)\, e^{ia/f_a} \approx (f_a + \rho + ia)$, where ρ is the boson associated to the "radial" excitations of the field and a is the axion. When we rewrite $\mathcal{L}_{PQ}$ using this parameterization, we find out that Q and ρ gain a mass of order $m_Q \sim m_\rho \sim f_a$. However, there is no mass term for the axion, as we would expect of a GB. On the other hand, since $U(1)_{PQ}$ is explicitly broken at quantum level, we know that the axion is instead a pGB, and has a very light mass m_a ($\propto 1/f_a$), that is of the same order of magnitude as that of the DFSZ axion, as it must also obey Eq. (3.10).

It is worth to highlight that the KSVZ axion only couples to the exotic quark Q and all the couplings to SM particles happen at loop level, unlike the DFSZ axion that couples to SM fermions at tree level through the Yukawa couplings with the Higgs doublets.

3.4. Heavy axion models

Up to now, I have discussed the predominant models of axion: the invisible axion models. I have commented that these models predict a very light axion that couples extremely weakly to SM particles. In the following sections we discussed that we can constrain the parameter space of the axion through its effective couplings to SM particles. In particular, the best constraints stem from the effective coupling to photons, that set the following upper and lower limits for the scale of the axion [22]: $f_a \sim 10^9 - 10^{12}$ GeV. From Eq. (3.10) these can be translated into limits for the mass of the axion: $m_a \sim 10^{-5} - 10^{-2}$ eV.

For a long time, it was thought that the invisible axion models were the only possible models that could solve the Strong CP problem. Nevertheless, recently much heavier axions with low f_a scales are starting to be considered. These new models are commonly called *heavy axion models*.

The original PQ axion as well as all invisible axion models assume that the gauge group of Nature is the SM one, $SU(3)_C \times SU(2)_L \times U(1)_Y$. In heavy axion models instead the strong interacting sector is enlarged beyond QCD (and contains the latter). This results in a value of the product $m_a f_a$ which is much larger than that in Eq. (3.10), softening and enlarging the allowed parameter space. The idea of these models comes from *technicolor* theories and their variants.

The properties of these models go beyond the scope of this work and they will no longer be developed here. The relevant aspect is that now a much larger region of the axion parameter space (that of axion-like-particles) may also solve the Strong CP problem.

4. EFFECTIVE LAGRANGIAN FOR AXIONS AND ALPS

4.1. Effective couplings to vector bosons

In this section, I construct an effective Lagrangian that describes the couplings between the axion or axion-like-particles (ALPs) and the gauge vector bosons of the SM. An ALP is a spin zero boson, pGB of some unknown symmetry, and thus it couples mainly derivative, as the axion. The difference between an axion and an ALP is simple, that the latter does not aim to solve necessarily the Strong CP problem. Otherwise, the phenomenology is similar. All the discussion of this section and the following ones will not only apply to axions, but also to ALPs. Thus, although this work is focused on the axion, all the experimental constraints on effective couplings for the axion also exclude the same part of the area of the ALPs' parameter space.

The importance of the effective field theories lies in their power to describe the low-energy limit of a model, where low energy is referred to some energy scale Λ (in our problem, f_a), considering only relevant degrees of freedom, while the high-energy ones are "integrated out": their effects are only visible in the effective couplings and operators.

In order to do that, first we have to go one step back and look at the divergence of the current associated to the PQ symmetry: j^{μ}_{PQ}. For the case of true axions discussed previously, the axion couplings may also be anomalous in the QED sector too. In the DFSZ axion, this second anomaly is generated by the SM quarks, that have electromagnetic charge. However, it may also exist in the KSVZ axion if the exotic quark Q has electric charge too. Therefore, the two anomalous terms can be parameterized by the coefficients E and N as follows [29]:

$$\partial_\mu j^\mu_{PQ} = N\frac{\alpha_s}{4\pi} G^a_{\mu\nu}\tilde{G}^{a\mu\nu} + E\frac{\alpha_{em}}{4\pi} F_{\mu\nu}\tilde{F}^{\mu\nu} \,. \tag{4.1}$$

The value of the *anomalous coefficients* N and E depends on the representation of the quarks that are charged under $U(1)_{PQ}$ in the gauge group of the SM: $SU(3)_C \times SU(2)_L \times U(1)_Y$. We denote this representation as $R_Q = (C_Q, I_Q, Y_Q)$. C_Q is the representation of the quark Q under $SU(3)_Q$; I_Q is the representation under $SU(2)_L$; and, finally, Y_Q is the hypercharge of the quark. Notice that, if $I_Q = 1$ (the quark is a singlet of $SU(2)_L$) the hypercharge coincides with the electric charge of the quark q_Q. Using this notation, N and E are computed as follows:

$$N = \sum_Q 2(\chi_L - \chi_R) T(C_Q) \,, \qquad E = \sum_Q 2(\chi_L - \chi_R) q_Q^2 \,, \tag{4.2}$$

where the sum runs over all the quarks that are charged under $U(1)_{PQ}$, $\chi_{L,R}$ are the PQ charges of the quarks, and $T(C_Q)$ is the colour index of the representation C_Q of $SU(3)_C$. In general, we can take the convention: $|\chi_L - \chi_R| = 1$. Notice that for $C_Q = 3$ (the fundamental representation), the coefficient of the colour chiral anomaly coincides with the previous result in Eq. (2.34): $T(C_Q = 3) = 1/2$.

On the other hand, the axion couples at tree level with the quarks that are charged under the PQ symmetry via a term in the Lagrangian: $\sim a\overline{\psi}\gamma^5\psi \subset \mathcal{L}$. This term allows the axion to couple to the PQ current j^μ_{PQ}, so the next interaction between an axion and a pair of photons/gluons becomes possible at 1-loop order:

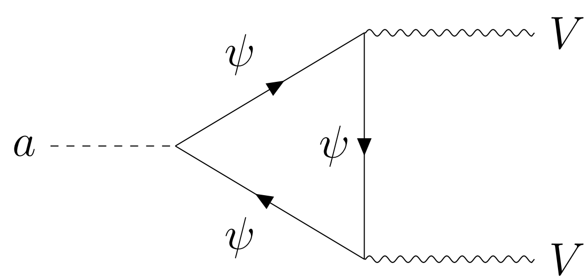

FIG. 8. Leading order coupling between the axion and a pair of vector bosons. This coupling stem from the anomalous term of the PQ current. Given Eq. (4.1) for the divergence of the current: $V = \gamma\,, g$.

When the quarks running in the loop in Fig. (8) are integrated out, the effective couplings that stem from this diagram are given by the following effective Lagrangian [30]:

$$\mathcal{L}^{eff} = \mathcal{L}^{SM} + \frac{1}{2}\partial_\mu a \partial^\mu a + \frac{1}{2}m_a^2 a^2 - \frac{1}{4}g_{agg} a G^a_{\mu\nu}\tilde{G}^{a\mu\nu} - \frac{1}{4}g_{a\gamma\gamma} a F_{\mu\nu}\tilde{F}^{\mu\nu}\,, \tag{4.3}$$

where the effective coupling constants g_{agg} and $g_{a\gamma\gamma}$ are defined as:

$$g_{agg} \equiv \frac{\alpha_s}{2\pi f_a} N\,, \qquad g_{a\gamma\gamma} \equiv \frac{\alpha_{em}}{2\pi f_a} E\,. \tag{4.4}$$

Notice that the two effective couplings $\sim aF\tilde{F}$ and $\sim aG\tilde{G} \subset \mathcal{L}^{eff}$ are dimension 5 operators, so they are suppressed by one power of the axion scale: $\sim 1/f_a$. Usually, the axion scale is redefined as: $f_a \to f_a/N$. This is done because, unlike the coupling to photons, the coupling to gluons has always to be present in every axion models in order to solve the Strong CP problem.

These effective couplings are model-dependent: they depend on the coefficients E and N, that are different for each model. However, these couplings also receive a contribution that does not depend on the specific axion model that is being used. These contributions stem from the mixing of the axion with the π_0 and η mesons, at energies below the QCD confinement scale $m_a < \Lambda_{QCD}$. For example, due to this mixing, the coupling to photons gain a second constant contribution [29]:

$$g_{a\gamma\gamma} = \frac{\alpha_{em}}{2\pi f_a}\left(\frac{E}{N} - 1.92(4)\right) = \frac{m_a}{\text{eV}}\frac{2.0}{10^{10}\ \text{GeV}}\left(\frac{E}{N} - 1.92(4)\right) . \tag{4.5}$$

The axion's (and ALPs') effective coupling to photons in Eq. (4.5) is the most experimentally constrained effective coupling. This is due to a mechanism called *Primakoff conversion* [32], illustrated in Fig. 9. Briefly, the effect consists on the resonant conversion of ALPs from/to photons enhanced by the presence of a intense magnetic field. In consequence, axion physics are also very important in astrophysics for light axions, e.g. those of the invisible axion models. Thanks to the Primakoff conversion, ALPs could contribute very effectively to the loss of energy in stars [33], affecting to a lot of astrophysical events. Some of the consequences would be an increase of the solar neutrino flux, a reduction of the helium-burning lifetime of stars, an accelerated white-dwarf cooling, and a reduction of number the supernovae, etc. Therefore, the observation (or lack of observation) of these events allows us to establish strong bounds for the ALPs' coupling to photons, for light axions and ALPs.

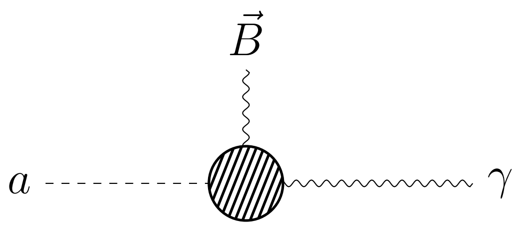

FIG. 9. Diagram representation of the photon-axion Primakoff conversion in the presence of a magnetic $\vec{B}$.

Let us consider the expression for the coupling constant to photons $g_{a\gamma\gamma}$ as it is written in Eq. (4.5). In Fig. 10 we show the regions of the plane $g_{a\gamma\gamma} - m_a$ that have been already excluded [29]. It has to be noticed that some of these constraints, such as HDM (Hot Dark Matter), assume an invisible axion model. Outside bound some of the constraints do not hold for ALPs nor heavy axion models.

Experimental tests that have been carried allow us to set strong constraints on the scale of the axion f_a and, from Eq. (3.10) $m_a \propto f_a^{-1}$, on its mass. Particularly, the upper limit on m_a comes from axion detection experiments, which are commented below. However, the lower limit applies only if the axion is assumed to constitute all the dark matter that have been detected in many astrophysical events [34]. From cosmological observations [35] it is known that the large structures in the universe were formed in a "bottom-up" scenario, that could be explained by the presence of *cold* dark matter (non-relativistic DM) in the structure

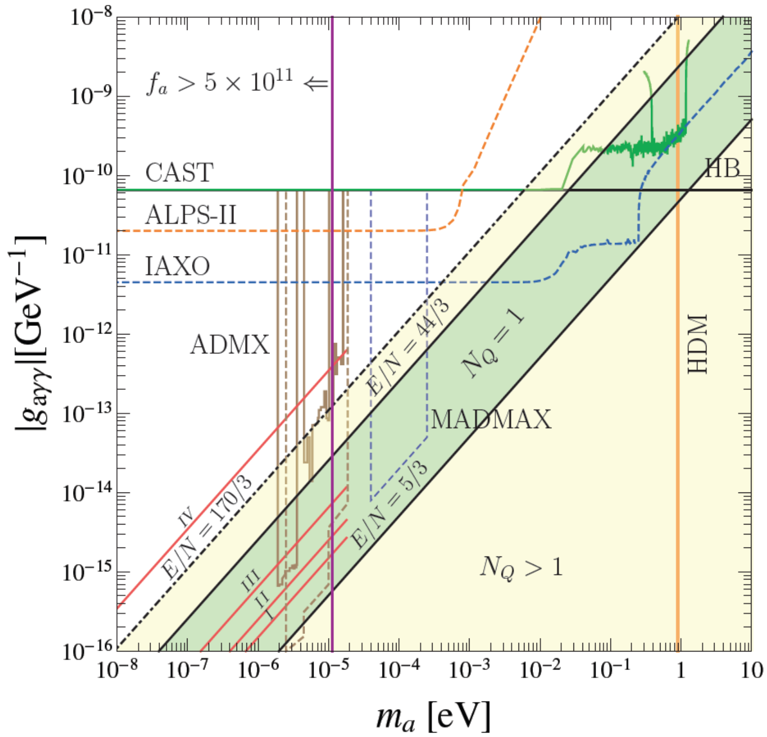

FIG. 10. Regions of the plane $g_{a\gamma\gamma}-m_a$ that are experimentally allowed for some axion models. The green region stems from the KSVZ axion with only one representation R_Q (one exotic quark), while the yellow region corresponds to the KSVZ model for several exotic heavy quarks Q (with different representations R_Q). The red lines correspond to different models of the DFSZ axion. Coloured continuous lines indicate those regions of the plane that are experimentally excluded. Dashed lines indicate the expected sensitivity for future axion detection experiments: ALPS-II, IAXO and MADMAX. The experimental data that have been included correspond to the experiments CAST and ADMX. Constraints that come from astrophysical observations are as well included, such as the counting of stars in the horizontal branch (HB) and the limit of hot dark matter (HDM) for the invisible axion. Figure extracted from Ref. [29].

formation epoch. For $m_a < 10^{-5}$ eV, the axion alone could not explain of the amount of cold dark matter that has been measured.

Some of the excluded regions in Fig. 10 stem from astrophysical observations. For example, HDM is a constraint from hot dark matter [36] and HB comes from the counting of stars in the horizontal branch [37].

Other regions are excluded from direct axion detection experiments. Most of these experiments try to take advantage of the Primakoff effect that we described above. These detection experiments can be mainly classified in two types: *axion helioscopes* and *microwave cavity experiments.*

Instead of computing the energy loss in stars due to axion emission fluxes, axion helioscopes try to measure directly these fluxes. These detectors aim to measure axion produced inside the Sun [38]. They would be produced through the two-photon effective coupling and immediately would escape from the interior of the Sun. Later, they would reach the detector, which has a very strong magnetic field inside it, and would transform back into photons via the reverse Primakoff conversion effect. One of the main axion helioscopes is CAST (CERN Axion Solar Telescope) [39], whose constraints are shown in Fig. 10. Additionally, in the same figure it is shown the expected sensitivity of the future axion helioscope experiment IAXO (International Axion Observatory) [40].

Microwave cavity experiments consist on Fabry-Perot optical cavities that are permeated by a strong static magnetic field. These experiments aim to measure DM galactic halo axions, that would be resonantly converted into a quasi-monochromatic microwave signal. They are tunable, and the axion signal is expected to be maximized when the frequency of the cavity coincides with the axion rest mass. One example of these experiments is ADMX (Axion Dark Matter eXperiment) [4]. The future experiment MADMAX (Magnetized Disc and Mirror Axion Experiment) [41] has to be highlighted too: it is not exactly a Fabry-Perot optical cavity, but is based on the same principle. The sensitivity expected for MADMAX is shown in Fig. 10.

Finally, the so-called *light shining through a wall* experiments are to be noted. One example is the future experiment ALPS-II [42]. The idea behind is similar to that for axion helioscopes. However, instead of measuring the solar axion flux, the aim is to measure an axion flux generated in the laboratory. This flux is generated by a laser, whose photons are converted into axions thanks to a magnetic field. The laser is pointing towards a wall, that axions can easily cross. Behind the wall there is an axion detector that aim to measure the axions using the same method as the axion helioscopes. Notice that these experiments require photon-axion conversion to happen twice, so the sensitivity is smaller $\propto g_{a\gamma\gamma}^2 \sim 1/f_a^2$.

However, if we look back to Eq. (4.5) we can notice something very interesting. If there was some specific axion or ALP model that satisfies $E/N \approx 1.92$, the model-dependent and model-independent terms of the photon coupling below Λ_{QCD} would cancel partially, resulting in strongly suppressed effective coupling to photons. These models are called *photophobic axion* [43]. For example, this happens in the KSVZ axion model, assuming two exotic heavy quarks whose representations R_Q are $(3, 3, -\frac{1}{3}) \oplus (\overline{6}, 1, -\frac{1}{3})$, that gives rise to $E/N = 23/12 \approx 1.92$. On the one hand, it is true that this cancellation of the coupling to two photons requires fine-tuning and an ad-hoc election of the representation of the quarks. On the other hand, it constitutes an example showing that the strong constraints that are usually considered for m_a and f_a can become more flexible. In other words, there can be axions that still solve the Strong CP problem (or ALPs from different theories) in other ranges of masses and couplings, which is of great importance for the detection experiments.

For all these reasons, it is also important to analyze the possible couplings to EW gauge bosons, since they may become the most relevant ones for some of these models. Particularly, LHC and collider searches of axions and ALPs could take great advantage of these possible couplings, that may be detected in many signals, for example, through their impact on meson decays. Ignoring the model-independent contribution (that comes from the mixing with the π_0 and η mesons), the couplings between ALPs and the gauge bosons of the SM can be parameterized by the three following gauge invariant 5-dimensional operators [44]:

$$\mathcal{L}^{eff} \supset -\frac{1}{4} g_{agg} a G^a_{\mu\nu} \tilde{G}^{a\mu\nu} - \frac{1}{4} g_{aWW} a W^a_{\mu\nu} \tilde{W}^{a\mu\nu} - \frac{1}{4} g_{aBB} a B_{\mu\nu} \tilde{B}^{\mu\nu} \,, \tag{4.6}$$

where $W^a_{\mu\nu}$ and $B_{\mu\nu}$ are the field strength tensors of the gauge groups $SU(2)_L$ (weak isospin) and $U(1)_Y$ (weak hypercharge) respectively, before EWSB. The effective coupling constant g_{agg} is defined as in Eq. (4.4). The other coupling constants are defined in a similar way:

$$g_{aWW} \equiv \frac{\alpha_W}{2\pi f_a} L \,, \qquad g_{aBB} \equiv \frac{\alpha_B}{2\pi f_a} P \,, \tag{4.7}$$

where L and P are two model-dependent coefficients that characterize the effective coupling.

After EWSB, the Z boson and the photons (that together with the $W^{\pm}$ bosons are the physical EW bosons) appear as a linear combination of the W_3 and B bosons. These combinations depend on a parameter θ_W that is called *weak angle*. Using the compact notation $c_W \equiv \cos\theta_W$ and $s_W \equiv \sin\theta_W$, we can express the photon and the Z as:

$$\begin{pmatrix} \gamma \\ Z \end{pmatrix} = \begin{pmatrix} c_W & s_W \\ -s_W & c_W \end{pmatrix} \begin{pmatrix} B \\ W_3 \end{pmatrix} . \tag{4.8}$$

Moreover, the W^+ and W^- appear as a combination of the W_1 and W_2 as:

$$W^{\pm} = \frac{1}{\sqrt{2}} \left(W_1 \mp i W_2 \right) . \tag{4.9}$$

When these expressions are substituted in the Lagrangian (4.6), we obtain the couplings to the physical gauge bosons (that are valid for energies below v) [44]:

$$\begin{aligned} \mathcal{L}^{eff} \supset & -\frac{1}{4} g_{agg} a G^a_{\mu\nu} \tilde{G}^{a\mu\nu} - \frac{1}{2} g_{aWW} a W^+_{\mu\nu} \tilde{W}^{-\mu\nu} \\ & -\frac{1}{4} g_{a\gamma\gamma} a F_{\mu\nu} \tilde{F}^{\mu\nu} - \frac{1}{4} g_{a\gamma Z} a F_{\mu\nu} \tilde{Z}^{\mu\nu} - \frac{1}{4} g_{aZZ} a Z_{\mu\nu} \tilde{Z}^{\mu\nu} \,, \end{aligned} \tag{4.10}$$

where the constants g_{aZZ} and $g_{a\gamma Z}$ are associated to the effective couplings of the axion or ALP to two Z bosons and one photon and one Z boson, respectively. Then, the constants that describe the couplings to EW bosons are expressed as:

$$\begin{aligned} g_{a\gamma\gamma} &= \frac{1}{2\pi f_a}\alpha_{em}E\,, \qquad & g_{aWW} &= \frac{1}{2\pi f_a}\frac{\alpha_{em}}{s_W^2}L \\ g_{aZZ} &= \frac{1}{2\pi f_a}\frac{\alpha_{em}}{s_W^2 c_W^2}Z\,, \qquad & g_{a\gamma Z} &= \frac{1}{2\pi f_a}\frac{\alpha_{em}}{s_W c_W}2R\,, \end{aligned} \tag{4.11}$$

where Z and R are two coefficients that characterize their respective couplings. Notice that $\alpha_{em} = \alpha_W s_W^2 = \alpha_B c_W^2$.

It should be noticed that those four effective couplings (4.11) arise from only two terms in the Lagrangian before EWSB (4.6). Therefore, only two out of the four coefficients E, Z, R and L can be linearly independent. Particularly, E, Z and R can be expressed as a function of L and P as follows:

$$E = L + P\,, \qquad Z = Lc_W^4 + Ps_W^4\,, \qquad R = Lc_W^2 - Ps_W^2\,. \tag{4.12}$$

This property of the effective couplings to EW bosons if very useful, because it can be used to set new constraints for one coupling without the need of measuring it directly. For example, the constraints on the coupling to photons, that is most constrained of all of them, can be used to set new bounds on the others, that are much more difficult to measure. A word of caution: this is a tree-level statement, and modified weights are expected at loop-level.

Finally, it should be commented that these constants (4.11) represent only the model-dependent contribution to the coupling to EW bosons. They also receive a model-independent contribution from the mixing of the axion (or ALP) with the π_0 and η mesons below Λ_{QCD}. The calculation of these contributions will not be further discussed on this work, but they can be found in Ref. [44].

4.2. Loop-induced couplings

All possible effective couplings in $\mathcal{L}^{eff}$ will mix and contribute to each other at the loop level. All the couplings that are allowed by the symmetries of the problem are generated, even if we assume that they are not present at tree-level. Phenomenologically, this feature of the effective field theories is very useful, since it can be used to establish new constraints for tree-level couplings based on their impact at the loop level on a different effective coupling. Therefore, it is crucial to study the loop-induced contributions that appear on those couplings that are more easily measurable, such as the coupling to photons.

In this section, the one-loop induced coupling of the axion to photons stemming from a tree-level coupling to fermions is computed. The computation existed in the literature for on-shell ALPs; we extend it to off-shell ALPs as this will be relevant for experimental searches, e.g. collider ALPs searches.

The effective coupling between the axion and the fermions, at tree-level, is given by the following flavour-diagonal 5-dimensional operator [46]:

$$\mathcal{L}^{eff} \supset \sum_{\psi} c_\psi \frac{\partial_\mu a}{f_a} \left(\overline{\psi}\gamma^\mu\gamma^5\psi\right) , \tag{4.13}$$

where c_ψ is the coefficient that characterizes the strength of the coupling. The Feynman rule associated to this effective vertex is given by:

$$-i\frac{c_\psi}{f_a}(ip_\mu)\gamma^\mu\gamma^5 = \frac{c_\psi}{f_a}\not{p}\gamma^5 , \tag{4.14}$$

where p_μ is the momentum of the axion.

Notice that this is a derivative coupling to the fermions, as expected for their GB origin. For the coupling to EW bosons the property that all dominant couplings are derivative was not shown explicitly, but it can be appreciated when we realize that $F\tilde{F}$ can be rewritten as a total derivate ($\partial_\mu K^\mu$, for some vector K^μ) for any gauge group, as in Eq. (2.3).

Let us consider the coupling c_ψ in Eq. (4.13). At one-loop-level, it may induce an axion-$\gamma\gamma$ coupling as illustrated in Fig. 11.

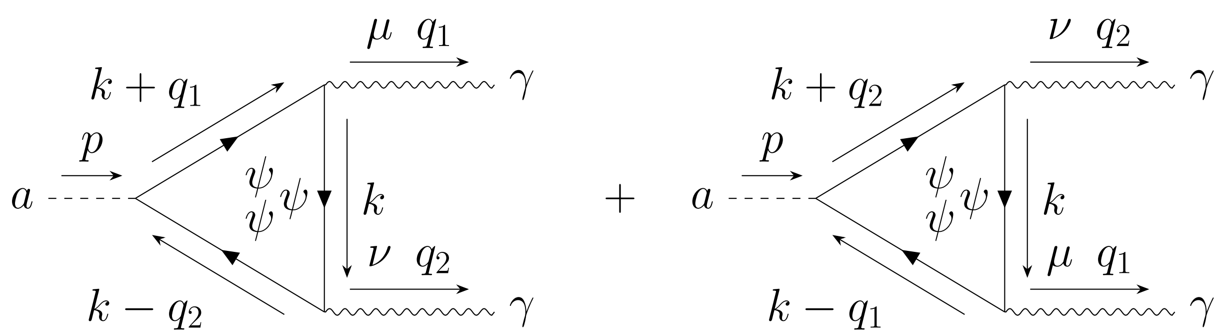

FIG. 11. One-loop induced coupling to two photons through a tree-level effective coupling to charged fermions.

Notice that these diagrams are quite similar to those in Fig. 2, that give rise to the axial anomaly. Therefore, they can be computed following almost the same steps followed in Sect. 2.2. However, this time we cannot neglect the mass of the fermions in the loop.

Let us start computing only the first diagram. The amplitude of the process is given by the following expression:

$$-i\mathcal{M} = -i\mathcal{M}^{\mu\nu}\varepsilon^*_\mu(q_1)\varepsilon^*_\nu(q_2)\,, \tag{4.15}$$

where $\varepsilon^*_\lambda(q)$ is the polarization vector of the photons. $\mathcal{M}^{\mu\nu}$ is computed as:

$$-i\mathcal{M}^{\mu\nu} = (-1)(ieQ_\psi)^2\frac{c_\psi}{f_a}\int\frac{\mathrm{d}^4k}{(2\pi)^4}\,\mathrm{Tr}\left[\not{p}\gamma^5\frac{i(\not{k}-\not{q}_2+m)}{(k-q_2)^2-m^2}\gamma^\nu\frac{i(\not{k}+m)}{k^2-m^2}\gamma^\mu\frac{i(\not{k}+\not{q}_1+m)}{(k+q_1)^2-m^2}\right]\,, \tag{4.16}$$

where m is the mass of the fermions. Then:

$$\mathcal{M}^{\mu\nu} = \frac{c_\psi e^2Q_\psi^2}{f_a}\int\frac{\mathrm{d}^4k}{(2\pi)^4}\,\mathrm{Tr}\left[\not{p}\gamma^5\frac{(\not{k}-\not{q}_2+m)}{(k-q_2)^2-m^2}\gamma^\nu\frac{(\not{k}+m)}{k^2-m^2}\gamma^\mu\frac{(\not{k}+\not{q}_1+m)}{(k+q_1)^2-m^2}\right]\,. \tag{4.17}$$

As it happened in Sect. 2.2, we are dealing with a momentum integral that may diverge. It is then necessary to solve it choosing an appropriate regularization method. We have used dimensional regularization. Therefore, once again, k (the momentum running in the integral) has to be decomposed as $k = k_\parallel + k_\perp$ where $k_\parallel$ only has non-zero components in the physical dimensions and $k_\perp$ only has non-zero components in the extra $d-4$ dimensions (it commutes).

Again, in a similar way to the analysis in Sect. 2.2, Eq. (2.23):

$$\not{p}\gamma^5 = (\not{k}+\not{q}_1-m)\gamma^5 + \gamma^5(\not{k}-\not{q}_2-m) - 2\gamma^5(\not{k}_\perp-m)\,. \tag{4.18}$$

The contribution of the two first terms in this expression vanishes, due to the same reasons exposed in Sect. 2.2, Eq. (2.21). We are then left with the following expression:

$$\mathcal{M}^{\mu\nu} = -\frac{2c_\psi e^2Q_\psi^2}{f_a}\int\frac{\mathrm{d}^dk}{(2\pi)^d}\,\mathrm{Tr}\left[\gamma^5(\not{k}_\perp-m)\frac{(\not{k}-\not{q}_2+m)}{(k-q_2)^2-m^2}\gamma^\nu\frac{(\not{k}+m)}{k^2-m^2}\gamma^\mu\frac{(\not{k}+\not{q}_1+m)}{(k+q_1)^2-m^2}\right]\,. \tag{4.19}$$

Again, the denominator can be rewritten introducing the Feynman parameter in the usual way:

$$\begin{aligned}&\frac{1}{[k^2-m^2]\,[(k-q_2)^2-m^2]\,[(k+q_1)^2-m^2]} = \\ &= \int_0^1\mathrm{d}x\int_0^{1-x}\mathrm{d}y\,\frac{2}{\left[k^2-m^2+xq_1^2+yq_2^2+2k(xq_1-yq_2)\right]^3}\quad.\end{aligned} \tag{4.20}$$

The momentum in the loop k can now be shifted as $k \to k - xq_1 + yq_2$, so that denominator can be rewritten as: $[k^2-\Delta]^3$, where:

$$\Delta \equiv m^2 - x(1-x)q_1^2 - y(1-y)q_2^2 - 2xyq_1q_2\,. \tag{4.21}$$

However, this time the numerator can be split in two different terms:

$$\begin{aligned} &\mathrm{Tr}\left[\gamma^5(\not{k}_\perp - m)(\not{k} - \not{q}_2 + m)\gamma^\nu(\not{k} + m)\gamma^\mu(\not{k} + \not{q}_1 + m)\right] = \\ &= \mathrm{Tr}\left[\gamma^5\not{k}_\perp(\not{k} - \not{q}_2 + m)\gamma^\nu(\not{k} + m)\gamma^\mu(\not{k} + \not{q}_1 + m)\right] \\ &- m\,\mathrm{Tr}\left[\gamma^5(\not{k} - \not{q}_2 + m)\gamma^\nu(\not{k} + m)\gamma^\mu(\not{k} + \not{q}_1 + m)\right]\,. \end{aligned} \tag{4.22}$$

Let us call $\mathcal{M}_1^{\mu\nu}$ and $\mathcal{M}_2^{\mu\nu}$ the contribution of the first and the second term, respectively.

First, let us consider only the first term. The only way to produce a non-zero trace is to keep one factor of each γ^μ, γ^ν, $\not{q}_1$ and $\not{q}_2$. Also, we require one $\not{k}$ factor so that when multiplied by $\not{k}_\perp$ it results: $\not{k}\not{k}_\perp = (k_\perp)^2$. Therefore, all the products that keep the mass of the fermions, m, produce a zero trace, so we get exactly the same result that we computed in section 2.2 (in which we neglected the mass of the fermion):

$$\mathrm{Tr}\left[\gamma^5\not{k}_\perp(\not{k} - \not{q}_2 + m)\gamma^\nu(\not{k} + m)\gamma^\mu(\not{k} + \not{q}_1 + m)\right] = i4\epsilon^{\mu\nu\alpha\beta}q_{1\alpha}q_{2\beta}k_\perp^2\,. \tag{4.23}$$

The contribution of this term to the amplitude is then:

$$\mathcal{M}_1^{\mu\nu} = -\frac{c_\psi e^2 Q_\psi^2}{4\pi^2 f_a}\epsilon^{\mu\nu\alpha\beta}q_{1\alpha}q_{2\beta}\,. \tag{4.24}$$

On the other hand, the second term adds a new contribution. In order to produce a non-zero trace, we have to keep one factor γ^μ and γ^ν and two of the slashed momenta. Therefore, at the end the result is proportional to m^2:

$$-m\,\mathrm{Tr}\left[\gamma^5(\not{k} - \not{q}_2 + m)\gamma^\nu(\not{k} + m)\gamma^\mu(\not{k} + \not{q}_1 + m)\right] = -i4\epsilon^{\mu\nu\alpha\beta}q_{1\alpha}q_{2\beta}m^2\,. \tag{4.25}$$

Notice that this result is invariant under the shift $k \to k - xq_1 + yq_2$. Then, the contribution to the amplitude of the second term can be written as:

$$\mathcal{M}_2^{\mu\nu} = i\frac{16c_\psi e^2 Q_\psi^2 m^2}{f_a}\epsilon^{\mu\nu\alpha\beta}q_{1\alpha}q_{2\beta}\int_0^1 \mathrm{d}x\int_0^{1-x}\mathrm{d}y\int \mathrm{d}^d k\,\frac{1}{\left[k^2 - \Delta\right]^3}\,. \tag{4.26}$$

The integral over momentum k converges now in the limit $d \to 4$ and can be solved in spherical coordinates:

$$\int \frac{\mathrm{d}^d k}{(2\pi)^d}\frac{1}{[k^2 - \Delta]^3} = \frac{-i}{2(4\pi)^{d/2}}\frac{\Gamma(3 - d/2)}{\Delta^{3-d/2}} \overset{d\to 4}{=} \frac{-i}{32\pi^2}\frac{1}{\Delta}\,. \tag{4.27}$$

Then:

$$\mathcal{M}_2^{\mu\nu} = \frac{c_\psi e^2 Q_\psi^2}{4\pi^2 f_a}\epsilon^{\mu\nu\alpha\beta}q_{1\alpha}q_{2\beta}\int_0^1 \mathrm{d}x\int_0^{1-x}\mathrm{d}y\,\frac{2m^2}{m^2 - x(1-x)q_1^2 - y(1-y)q_2^2 - 2xyq_1q_2}\,. \tag{4.28}$$

Finally, the sum of both contributions results in:

$$\begin{aligned}\mathcal{M}^{\mu\nu} &= -\frac{c_\psi e^2 Q_\psi^2}{4\pi^2 f_a}\epsilon^{\mu\nu\alpha\beta}q_{1\alpha}q_{2\beta}\times \\ &\times\left[1-\int_0^1 \mathrm{d}x\int_0^{1-x}\mathrm{d}y\,\frac{2m^2}{m^2-x(1-x)q_1^2-y(1-y)q_2^2-2xyq_1q_2}\right]\,.\end{aligned} \tag{4.29}$$

Notice that this expression is again symmetric under the interchange $q_1 \leftrightarrow q_2$ and $\mu \leftrightarrow \nu$, so the second diagram adds an extra factor 2 in the amplitude.

This amplitude $\mathcal{M}^{\mu\nu}$ can be interpreted as an effective coupling to two photons. Comparing with the tree-level coupling to photons in Eq. (4.3), the amplitude associated to the process $a \to \gamma\gamma$ at tree-level is given by:

$$-i\mathcal{M}_0^{\mu\nu} = i g_{a\gamma\gamma}\epsilon^{\mu\nu\alpha\beta}q_{1\alpha}q_{2\beta} \;\Rightarrow\; \mathcal{M}_0^{\mu\nu} = -g_{a\gamma\gamma}\epsilon^{\mu\nu\alpha\beta}q_{1\alpha}q_{2\beta}\,. \tag{4.30}$$

Let us call $g^0_{a\gamma\gamma}$ to the coupling constant at tree-level. Comparing equations (4.29) and (4.30), the following expression for the full coupling to photons reads:

$$\begin{aligned}g_{a\gamma\gamma} &= g^0_{a\gamma\gamma} + \sum_\psi \frac{2c_\psi\alpha_{em}Q_\psi^2 N_C}{\pi f_a}\times \\ &\times\left[1-\int_0^1 \mathrm{d}x\int_0^{1-x}\mathrm{d}y\,\frac{2m_\psi^2}{m_\psi^2-x(1-x)q_1^2-y(1-y)q_2^2-2xyq_1q_2}\right]\,,\end{aligned} \tag{4.31}$$

where the sum runs over all fermions ψ that couple to the axion or ALP. Notice that, since the process is colour-independent, we have also included the colour degeneration for the quarks.

The integral over the Feynman parameters x and y is, in general, hard to compute. However, if we consider the specific case in which both photons are produced on-shell ($q_1^2 = q_2^2 = 0$ and $2q_1q_2 = p^2$) it simplifies, leading to:

$$g_{a\gamma\gamma} = g^0_{a\gamma\gamma} + \sum_\psi \frac{2c_\psi\alpha_{em}Q_\psi^2 N_C}{\pi f_a} B_1(m_\psi, p^2)\,, \tag{4.32}$$

where B_1 is defined as [46]:

$$B_1(m_\psi, p^2) = 1 - \frac{4m_\psi^2}{p^2}\left[f(m_\psi, p^2)\right]^2\,, \tag{4.33}$$

where

$$f(m_\psi, p^2) = \begin{cases} \arcsin\left(\frac{\sqrt{p^2}}{2m_\psi}\right) & \text{for } \sqrt{p^2} \le 2m_\psi\,, \\ \frac{\pi}{2} + \frac{i}{2}\log\left(\frac{\sqrt{p^2}+\sqrt{p^2-4m_\psi^2}}{\sqrt{p^2}-\sqrt{p^2-4m_\psi^2}}\right) & \text{for } \sqrt{p^2} > 2m_\psi\,. \end{cases} \tag{4.34}$$

In the limit $p^2 \gg m_\psi^2$ $B_1 \approx 1$, while $B_1 \approx -p^2/12m_\psi^2$ in the opposite limit $p^2 \ll m_\psi^2$.

B_1 takes in general complex values. However, if there is no interference with the SM, when we compute an observable, i.e. a cross section, the result will only depend on the modulus $|B_1|$ in the absence of interference. In order to get a better intuition about this function $|B_1|$ is drawn in Fig. 12, for the case in which the fermion is the top quark.

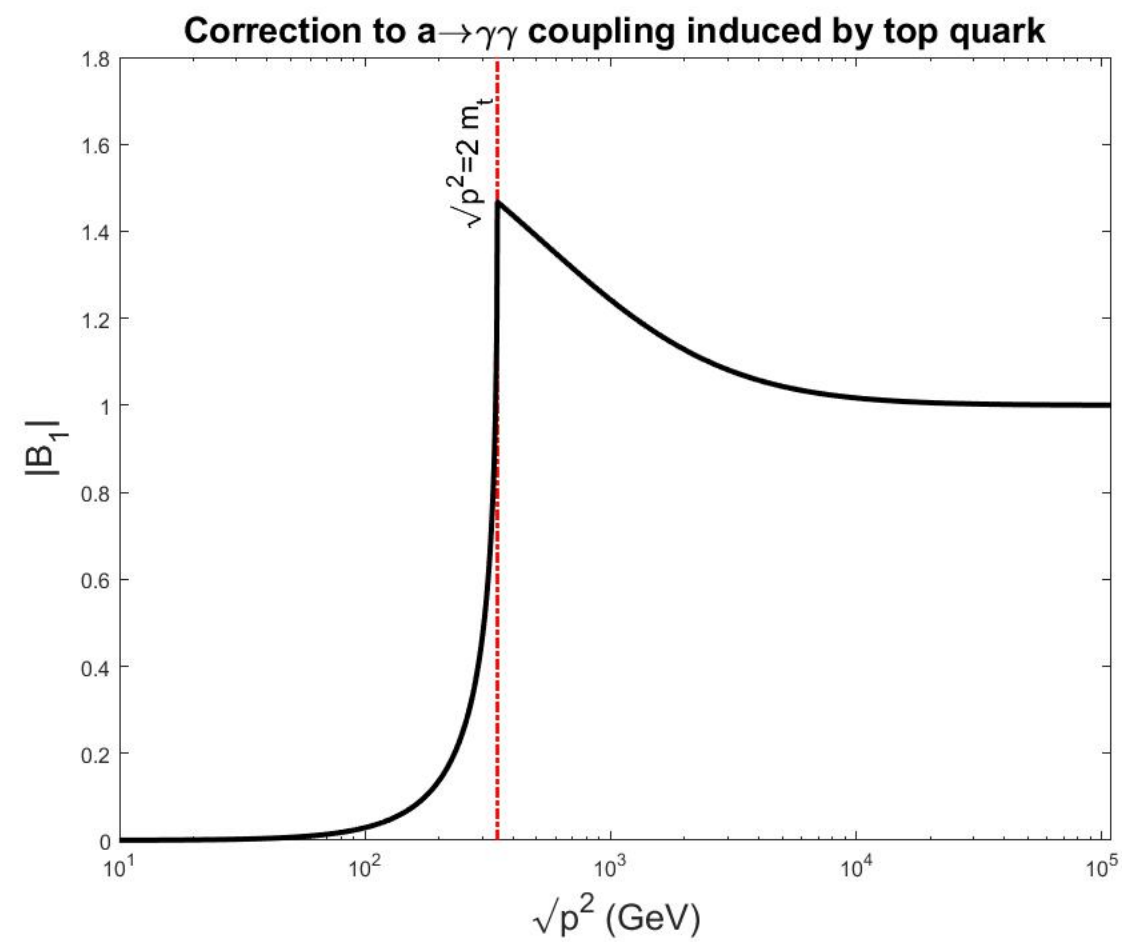

FIG. 12. Correction to $g_{a\gamma\gamma}$ induced by the top quark.

B_1 is similar to a step-function centered at $\sqrt{p^2} = 2m_t$: at energies below that value the fermion triangle loop barely contributes to $g_{a\gamma\gamma}$, but for energies much larger than $2m_t$ it gives a constant contribution.

Things become a bit different when you consider all SM electrically charged fermions. From the last result, we would expect a function with some steps at $2m_\psi$ for each fermion. Eq. (4.32) shows that the contribution of every fermion is averaged by c_ψ and Q_ψ^2 and thus, fermions with different electric charges have different weights. Assuming $c_\psi \approx 1$ for the effective coupling of every fermion at tree-level, we can expand:

$$\sum_{\psi} Q_{\psi}^2 B_1(m_{\psi}^2, p^2) = \frac{4}{9}\sum_{u,c,t} B_1(m_{\psi}^2, p^2) + \frac{1}{9}\sum_{d,s,b} B_1(m_{\psi}^2, p^2) + \sum_{e,\mu,\tau} B_1(m_{\psi}^2, p^2)\,. \tag{4.35}$$

Fig. 13 depicts the modulus of this expression as a function of $\sqrt{p^2}$.

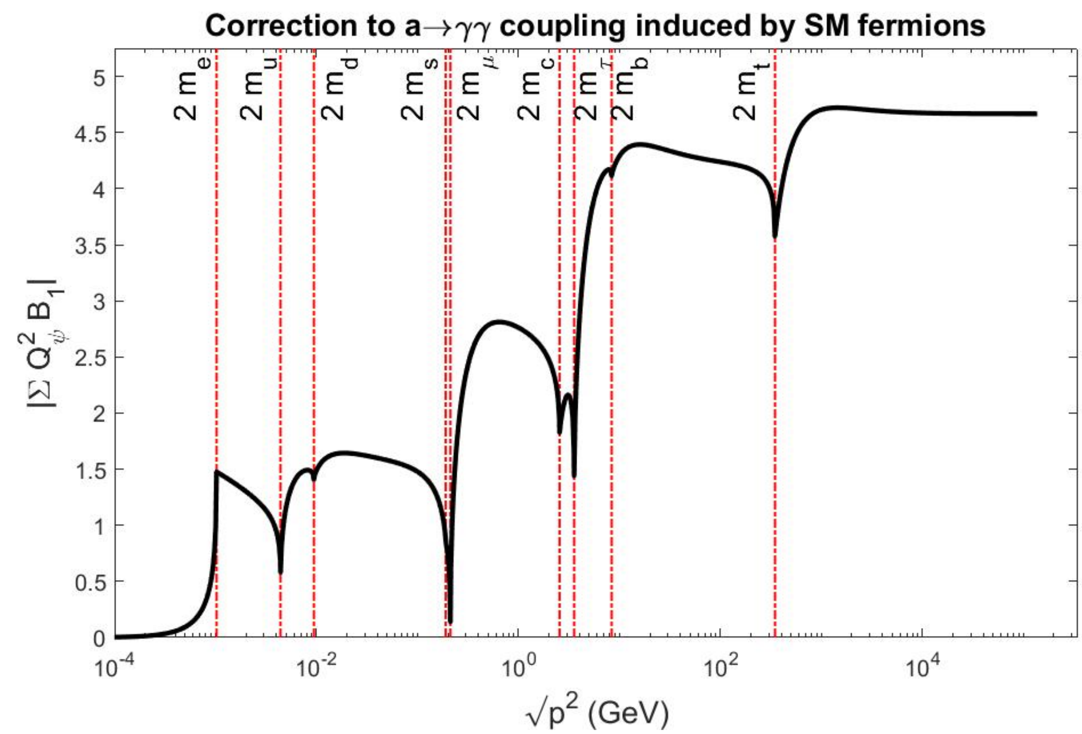

FIG. 13. Correction to $g_{a\gamma\gamma}$ induced by the all SM fermions in the approximation $c_\psi \approx 1$ for every fermion. The figure illustrates that for energies below $2m_e$ the fermions barely contribute, while for energies above $2m_t$ their contribution is a constant term. However, for energies between these values, the of sum of the individual contributions leads to cancellations and a richer substructure.

In the following section, we will see how these loop-induced contributions can be used to establish new constraints on axion tree-level effective couplings. In particular, we establish a new constraint on the lepton couplings based on their loop-induced contribution to the photon coupling.

4.3. New constraints: non-resonant searches

The detection methods discussed in Sect. 4.1 aim to find a signal of the axion when it is produced on-shell (on-resonance). Even searches at colliders aimed up to now to find a signal of an on-shell production of the axion or a resonant peak, that happens when an on-shell axion mediates a process in s-channel. However, Ref. [5] discussed a novel approach: *non-resonant axion searches*, that aim to find a "footprint" of the axion (or ALPs) when it is produced highly off-shell in colliders (particularly, in LHC). These searches try to take advantage of the derivate couplings of the ALPs, that are typical of pGB, whose strength increases with the energy. Thus, at the high energies of the particle colliders (such LHC), even if the ALP is not produced on resonance, the amplitude of the processes mediated by ALPs becomes substantial.

This novel approach is used here to establish a new constraint on the effective coupling of the axion to leptons, based on their loop-induced coupling to photons, that we discussed in the previous Sect. (4.32). This constitutes original work.

In order to show what this new approach consists of, let us consider the scattering process $gg \to a \to \gamma\gamma$, mediated by an axion in s-channel. See Fig. 14. The most likely process to produce it in pp colliders, like LHC, is the fusion of two gluons. For ALPs this is not mandatory, but it will be assumed here to be the case.

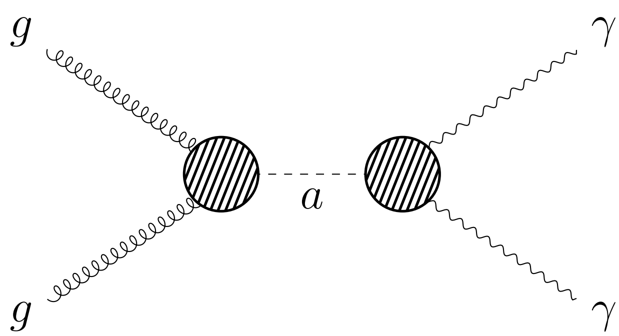

FIG. 14. Feynman diagram corresponding to the scattering process $gg \to a \to \gamma\gamma$ in s-channel.

Let us consider a two-coupling-at-a-time approach. First, no tree-level coupling to leptons will be considered. Instead, an effective Lagrangian for the axion of the form $\mathcal{L}^{eff} \supset -\frac{1}{4} g_{agg} G\tilde{G} - \frac{1}{4} g_{a\gamma\gamma} F\tilde{F}$ is assumed, where the axion only couples at tree-level to gluons and photons. Later, the coupling to photons will be fully replaced by an effective coupling to leptons.

The cross section σ of the scattering process in Fig. 14 can be easily computed. Moreover, since the process is expected to happen in particle colliders, at very high energies, the mass and the decay width of the axion can be safely neglected: $s \gg m_a^2, \Gamma_a m_a$. Then, $\sigma(gg \to a \to \gamma\gamma)$ is given by the following expression:

$$\sigma(gg \to a \to \gamma\gamma) = \frac{|g_{agg}|^2 |g_{a\gamma\gamma}|^2}{4096\pi} \frac{s^3}{(s - m_a^2)^2 + (\Gamma_a m_a)^2} \overset{s \gg m_a^2}{\approx} \frac{|g_{agg}|^2 |g_{a\gamma\gamma}|^2}{4096\pi} s \,. \tag{4.36}$$

As expected, in the high energy limit the cross section is proportional to s. In other words, the process becomes more likely for high energies. This behaviour stems from the derivative nature of the coupling of the pGBs. At this point, it has to highlighted that this result in Eq. (4.36) does not hold for arbitrarily high energies. In order to ensure the validity of the EFT, we must restrict the result to $\sqrt{s} \leq f_a$, otherwise our pertubative expansion in $\sqrt{s}/f_a$ would break since higher dimensional operators become relevant.

In the high energy limit, the cross section does not the depend on the mass of the axion: it only depends on its momentum squared: $s = p^2$. This feature is specially important when establishing new experimental constraints on the effective couplings. Since non-resonant searches do not assume a specific mass for the axion, they can be used to put new limits on the effective coupling constants that do not depend on m_a. Thus, they have the power to exclude huge areas in the parameter space of the axion. That is the main advantage of non-resonant searches.

The first work on this novel approach to axion phenomenology can be found in Ref. [5]. In that manuscript, this technique is applied to the Run 2 CMS data [47] (in LHC) to look for a signal of an ALP that couples to SM gauge bosons and Higgs bosons. Therefore, the tree level process described in (4.36) is possible. Specifically, they analyzed the events in which there are at least two photons in the final state. In order to ensure the high energy limit $s \gg m_a^2$, they imposed that these photons have to have an invariant mass $m_{\gamma\gamma}(= \sqrt{s})$ such that: $m_{\gamma\gamma} > 500$ GeV. With that filter, the approximation $s \gg m_a^2$ holds for ALP masses up to $m_a \leq 200$ GeV. The results were used to constrain the product $|g_{agg}||g_{a\gamma\gamma}|$. In particular, by choosing $g_{agg}^{-1} = 1$ TeV, the following upper limit was obtained (for any hypothetical ALP) [5]:

$$g_{a\gamma\gamma} \leq 0.080 \text{ TeV}^{-1} \qquad \text{at } 95\% \text{ C.L.} \tag{4.37}$$

This result is represented by the hatched are in Fig. (15), together with the current constraints on $g_{a\gamma\gamma}$. The figure includes resonant searches at: i) particle colliders (LHC and LEP); ii) beam dump experiments [48]; iii) the BaBar experiment [49] (USA) and iv) astrophysical observations such as supernova SN1987a [50]. The new area excluded by non-resonant data is quite large and the constraint holds up to $m_a \leq 200$ GeV.

On the other hand, as it was depicted in Sect. 4.2, all these constraints can be easily translated into constraints on the effective couplings to other particles, e.g. leptons. In order to do that, let us consider the case in which there is no tree-level coupling to photons. Instead, the axion couples at tree-level to leptons through the following Lagrangian:

$$\mathcal{L}^{eff} \supset -\frac{1}{4} g_{agg} G\tilde{G} + \sum_{e,\mu,\tau} \frac{c_l}{f_a} \partial_\mu a \left(\bar{l}\gamma^\mu\gamma^5 l\right) , \tag{4.38}$$

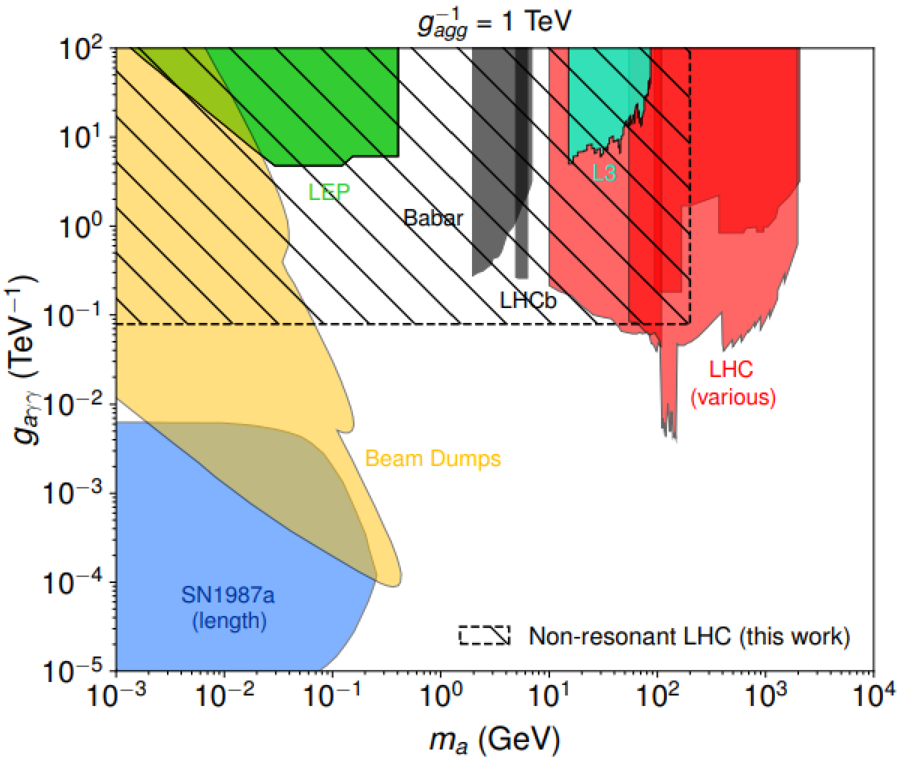

FIG. 15. Constraints on the effective coupling of ALPs to two photons. There are included those constraints that stem form searches at colliders, such as LHC and LEP; beam dump experiments; the BaBar experiment and those that come from astrophysical observations, such as suppernovae (SN1987a). Notice that it is also included the constraint from non-resonant searches of ALPs at LHC, that does not depend on the mass of the ALP. Figure extracted from Ref. [5].

and the coupling to photons in generated at 1-loop-level as discussed in Sect. 4.2.

In this work, we concentrate on tree-level axion-lepton couplings. Leptons are singlets of $SU(3)_C$, so that they do not introduce any correction at 1-loop level in the gluon effective vertex, unlike quarks. Furthermore, for those events in LHC that satisfy $m_{\gamma\gamma} > 500$ GeV, we can neglect the mass of the leptons and consider the limit $B_1 \approx 1$. We will assume safely that lepton flavour universality is satisfied for the effective coupling to ALPs, so that all their effective coupling constants are equal: $c_l \equiv c_e \approx c_\mu \approx c_\tau$.

The loop-induced coupling to photons that stems from this Lagrangian can be deduced from Eq. (4.32):

$$g_{a\gamma\gamma} = \frac{c_l}{f_a}\frac{6\alpha_{em}}{\pi}B_1\,. \tag{4.39}$$

From Eq. (4.37) and Eq. (4.39) we can now derive from non-resonant data the following constraint on the effective coupling between ALPs and charged leptons:

$$\frac{c_l}{f_a} \leq 5.3 \text{ TeV}^{-1} \qquad \text{at } 95\% \text{ C.L.} \tag{4.40}$$

This new bound is depicted as a hatched area in the plane $c_l/f_a - m_a$ in Fig. 16. The rest of the constraints depicted correspond to previous resonant searches. The latter include: i) in red, the searches of the Edelweiss collaboration [52] for ALPs produced in the Sun by the scattering process $\gamma e \to ea$ and other processes; ii) in purple, the constraints from the observation of Red Giant stars: ALPs could carry a cooling of the core of these stars, which would delay the burning of Helium and modify their brightness [53]; iii) in yellow, the searches of ALPs radiated by electrons in beam dump experiments [54]; iv) finally, in blue, searches in BaBar of the process $ee \to 4\mu$ [55].

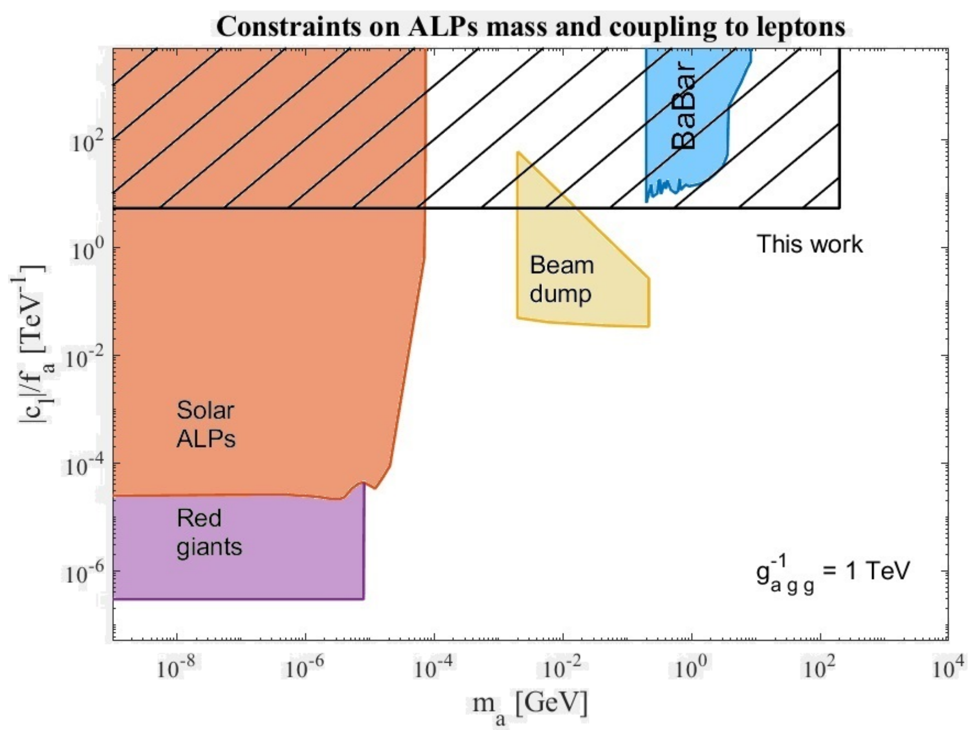

FIG. 16. Constraints on the effective coupling of ALPs to leptons assuming tree-level effective coupling of the ALP to gluons and to leptons. The constraint obtained in this work from non-resonant searches is depicted as a hatched region. Other excluded areas come from resonant searches as the BaBar experiment, beam dump searches for ALPs decaying into muons, solar ALPs searches and the observation of the evolution of red giant stars [51].

It should be pointed out that in the general case the constraint on Eq. (4.37) applies to the whole coupling constant $g_{a\gamma\gamma}$ in Eq. (4.32), that is made of the tree-level coupling to photons and the loop-induced corrections from fermions. In general, the constraint can be safely applied to each of the contributions assuming that there is no fine-tuning cancelation between them.

In summary, the non-resonant channels can be powerful tools to exclude large areas in the parameter space for axions and ALPs. They are independent of the axion mass as far as it is much lighter than the energy range of the data considered.

5. CONCLUSIONS

The Strong CP problem is one the main issues of the SM, which has remained unsolved for decades. We have reviewed how, due to instanton effects, the strong interactions should in all generality be a source of violation of CP because the QCD Lagrangian can *a priori* include a term $\overline{\theta}(\alpha_s/8\pi)G\tilde{G} \subset \mathcal{L}_{QCD}$, which has mass dimension four and is gauge invariant.

The issue can be understood as a naturalness problem, in the sense that it is puzzling why the $\overline{\theta}$ parameter is experimentally bound to be extremely small ($\leq 10^{-10}$). The Strong CP problem touches a fundamental characteristic of the SM, since the $\overline{\theta}$ parameter characterizes the vacuum of QCD.

A solution to this problem was proposed by Peccei and Quinn. In physics, the explanation through hidden symmetries of otherwise unnecessarily tiny values of parameters has been historically most fruitful. In order to justify the smallness of $\overline{\theta}$, Peccei and Quinn introduced a new global symmetry, $U(1)_{PQ}$, that is conserved at Lagrangian level but broken at quantum level. Moreover, the symmetry is spontaneously broken, and the axion appears as its (pseudo) Goldstone boson. This solution effectively results in a replacement of the $\overline{\theta}$ parameter by a dynamical field, the axion, that cancels the $\overline{\theta}$-term by choosing a specific vacuum expectation value. I have reviewed this proposal together with its realistic versions, called invisible axion models and heavy axion models. In these models, the axion is so weakly coupled to SM particles that it could have escaped detection in agreement with the present constraints on the parameter space for very light axions, or so heavy that the constraints on its scale and mass are weak.

On the other hand, the interest on the axion goes beyond particle physics. For instance, invisible axions could be one of the constituents or even the only constituent of dark matter. Thus, by solving a fundamental problem of particle physics, we could also find the answer to another fundamental problem in a totally different field of physics: astrophysics and cosmology.

We have also studied the phenomenology of the axion and, more generally, of ALPs. In the original part of this work, using effective Lagrangian techniques we first computed the one-loop level amplitudes to the axion-$\gamma\gamma$ coupling, induced by an axion tree-level coupling to fermions. This is the first time that this computation is performed for off-shell axions/ALPs.

Next, we focused on a novel recent approach proposed to look for ALP signals in particle colliders: non-resonant searches, which aim to look for a signal when the ALP is produced very off-shell, far away from its resonance. For instance, very light axions and ALPs can be produced at the much larger energies typical of LHC. Non-resonant searches take advantage of the derivative couplings of pGB, and their most powerful feature is that the expected signals do not depend on the mass of the ALPs, so they “sweep” huge areas of their parameter space. They have recently set new limits on their effective coupling to photons, studying the tree-level impact on LHC data of axion effective couplings. In this work, using the one-loop amplitudes that we derived, we have also established a new constraint on the effective coupling of the ALPs to leptons. This novel limit arises from the quantum-induced corrections of the coupling to leptons to the effective coupling to photons. This new bound constitutes a second original contribution.

The search for axions and ALPs is today a leading area of research in particle physics. A putative axion discovery can unravel one of the fundamental problems of the Standard Model of particle physics and, in addition, probably explain the nature of dark matter, whose understanding is also a scientific objective of first importance. The theoretical and experimental activity is in an intense growing phase. The discovery of the axion, if successful, may be one of the most important discoveries of 21st century science.

ACKNOWLEDGEMENTS

I want to express all my gratitude to Belén Gavela, for pushing me to give my best, sharing with me her motivation and dedication in research, and especially, for always supporting me in my learning. I would also like to thank Pablo Quilez, who has always been available to answer even the most stupid questions you can imagine. Thank you for your patience. I have also to thank Rachel Houzt and Meshkat Rajaee for their help with instantons, non-dissipative solutions, effective interactions and all these things that smart people like them easily understand, and I do not. Finally, thanks to Patricia, my family and friends, who have never stopped supporting me during this year. Thank you very much.

[1] C. A. Baker *et al.*: *An Improved experimental limit on the electric dipole moment of the neutron*. Phys. Rev. Lett. **97** (2006) 131801, arXiv:hep-ex/0602020 [hep-ex].

[2] Peccei, Roberto D.; Quinn, Helen R. (20 June 1977): *CP Conservation in the Presence of Pseudoparticles*. Physical Review Letters. **38** (25): 1440–1443

[3] Jihn E. Kim. *Light Pseudoscalars, Particle Physics and Cosmology*. Phys.Rept. **150** (1987) 1-177

[4]] S. J. Asztalos *et al.* (ADMX), Phys. Rev. **D69**, 011101 (2004), arXiv:astro-ph/0310042 [astro-ph].

[5] M. B. Gavela, J. M. No, V. Sanz, J. F. de Trocóniz (30 May 2019). *Non-Resonant Searches for Axion-Like Particles at the LHC*. arXiv:1905.12953 [hep-ph]

[6] Ta-Pei Cheng, Ling-Fong Li (1984): 10.2 The QCD Lagrangian and the simmetries of the strong interaction. *Gauge Theory of elementary particle physics* **291**. Oxford, Reino Unido: Clarendon Press.

[7] Michael E. Peskin, Daniel V. Schroeder. Chapter 19: Perturbation Theory Anomalies. *An Introduction To Quantum Field Theory*. Reading, USA: Addison-Wesley (1995). **661**. ISBN: 9780201503975, 0201503972.

[8] M. Kobayashi, T. Maskawa; Maskawa (1973). *CP-Violation in the Renormalizable Theory of Weak Interaction*. Progress of Theoretical Physics. **49** (2): 652–657.

[9] Maiani, L. *CP Violation in Purely Lefthanded Weak Interactions*. Phys.Lett. **62B** (1976) 183-186.

[10] E. Shabalin, Electric Dipole Moment of Quark in a Gauge Theory with Left-Handed Currents, Sov.J.Nucl.Phys. **28** (1978) 75.

[11] Gavela, M B, Le Yaouanc, A, Oliver, L, Pene, O, Raynal, J C, and Pham, T N. *CP violation induced by penguin diagrams and the neutron electron dipole moment*. Netherlands: N. p., 1982. Web. doi:10.1016/0370-2693(82)90756-0.

[12] Gavela, M.B., Le Yaouanc, A., Oliver, L. et al. Z. Phys. C - Particles and Fields (1984) 23: 251. https://doi.org/10.1007/BF01546193

[13] A. Czarnecki and B. Krause, contributions," Phys. Rev. Lett. **78**, 4339 (1997) [hepph/9704355].

[14] Dar, S. (2000). *The Neutron EDM in the SM : A Review*. arXiv:hep-ph/0008248

[15] V. Baluni, CP, Phys. Rev. D *19* (Apr, 1979) 2227–2230.

[16] M. Tanabashi et al. (Particle Data Group), Phys. Rev. D *98*, 030001 (2018).

[17] H. Stroeher. *Feasibility Study for an EDM Storage Ring*. Input to the European Particle Physics Strategy Update 2018-2020, ID:18.

[18] UKQCD Collaboration: A.C. Irving, C. McNeile, C. Michael, K.J. Sharkey, H. Wittig (2001). *Is the up-quark massless?* arXiv:hep-lat/0107023

[19] R. D. Peccei and H. R. Quinn, Phys. Rev. Lett. **38** (1977) 1440

[20] R. D. Peccei and H. R. Quinn, Phys. Rev. D **16** (1977) 1791.

[21] Jérémie Quevillon, Christopher Smith (2019). *Axions are blind to anomalies.* arXiv:1903.12559 [hep-ph]

[22] R. Peccei (2008). *The Strong CP problem and axions.* Lect. Notes Phys. **741** 3–17, [hep-ph/0607268].

[23] Dine, M.; Fischler, W.; Srednicki, M. (1981). *A simple solution to the strong CP problem with a harmless axion.* Phys. Lett. **B104** (3): 199–202.

[24] Zhitnitsky, A. (1980). *On possible suppression of the axion-hadron interactions.* Sov. J. Nucl. Phys. **31**: 260.

[25] Kim, J.E. (1979): *Weak-Interaction Singlet and Strong CP Invariance.* Phys. Rev. Lett. **43** (2): 103-107.

[26] Shifman, M.; Vainshtein, A.; Zakharov, V. (1980). *Can confinement ensure natural CP invariance of strong interactions?.* Nucl. Phys. **B166** (3): 493–506.

[27] M.B. Gavela, M. Ibe, P. Quilez, T. T. Yanagida (2018). *Automatic Peccei-Quinn symmetry.* arXiv:1812.08174 [hep-ph]

[28] Gaillard, M.K., Gavela, M.B., Houtz, R. et al. Eur. Phys. J. C (2018) **78**: 972. https://doi.org/10.1140/epjc/s10052-018-6396-6

[29] L. Luzio, F. Mescia y E. Nardi: *Redefining the Axion Window.* arXiv:1610.07593v2 [hep-ph] (2017).

[30] H. Georgi, D. B. Kaplan, L. Randall. *Manifesting the invisible axion at low energies.* Physics Letters B **169**(1986) 73-78. doi:10.1016/0370-2693(86)90688-X.

[31] Lattanzi, M. (2008). *Decaying Majoron Dark Matter and Neutrino Masses.* AIP Conference Proceedings. **966** (1): 163–169. arXiv:0802.3155

[32] Sikivie, P.; Tanner, D.; Van Bibber, Karl (2007). *Resonantly Enhanced Axion-Photon Regeneration.* Physical Review Letters. **98** (17): 172002. arXiv:hep-ph/0701198

[33] Raffelt, Georg (2008). *Astrophysical Axion Bounds.* Lect.Notes Phys. **741**: 51-71. arXiv:hep-ph/0611350

[34] Roos, M.: *Dark Matter: The evidence from astronomy, astrophysics and cosmology,* arXiv:1001.0316 [astro-ph.CO] (2010).

[35] Bertone, G.; Hooper, D.; Silk, J. (2005). *Particle dark matter: Evidence, candidates and constraints.* Physics Reports. **405** (5–6): 279–390. arXiv:hep-ph/0404175

[36] C. Patrignani *et al.* (Particle Data Group), Chin. Phys. **C40**, 100001 (2016).

[37] A. Ayala, I. Dominguez, M. Giannotti, A. Mirizzi, and O. Straniero, Phys. Rev. Lett. **113**, 191302 (2014), arXiv:1406.6053 [astro-ph.SR].

[38] D. Lazarus, G. Smith, R. Cameron, A. Melissinos, G. Ruoso, *et. al., A Search for solar axions*, Phys.Rev.Lett. **69** (1992) 2333-2336.

[39] V. Anastassopoulos *et al.* (CAST), Nature Phys. (2017), 10.1038/nphys4109, arXiv:1705.02290 [hep-ex].

[40] I. G. Irastorza *et al.*, JCAP **1106**, 013 (2011), arXiv:1103.5334 [hep-ex].

[41] A. Caldwell, G. Dvali, B. Majorovits, A. Millar, G. Raffelt, J. Redondo, O. Reimann, F. Simon, and F. Steffen (MADMAX Working Group), Phys. Rev. Lett. **118**, 091801 (2017), arXiv:1611.05865 [physics.ins-det].

[42] R. Bähre *et al.*, JINST **8**, T09001 (2013), arXiv:1302.5647 [physics.ins-det].

[43] L. D. Luzio, F. Mescia, and E. Nardi, *Window for preferred axion models*, Phys. Rev. **D96** no. 7, (2017) 075003, 1705.05370.

[44] G. Alonso-Álvarez, M.B. Gavela, P. Quilez (2018). *Axion couplings to electroweak gauge bosons.* arXiv:1811.05466 [hep-ph]

[45] N. Craig, A. Hook, and S. Kasko, *The Photophobic ALP*, JHEP 09 (2018) 028, arXiv:1805.06538 [hep-ph].

[46] Bauer, M., Neubert, M. & Thamm, A. *Collider probes of axion-like particles*, J. High Energ. Phys. (2017) 2017: 44. https://doi.org/10.1007/JHEP12(2017)044

[47] A. M. Sirunyan*et al.* [CMS Collaboration], JHEP **1809** (2018) 101 [arXiv:1803.10093 [hep-ex]].

[48] Babette Döbrich (2017). *Axion-like Particles from Primakov production in beam-dumps.* arXiv:1708.05776 [hep-ph]

[49] Aubert, B.; Bazan, A., *et al.* (2002). *The BABAR detector.* Nuclear Instruments and Methods in Physics Research Section A: Accelerators, Spectrometers, Detectors and Associated Equipment. **479** (1): 1–116. arXiv:hep-ex/0105044

[50] Kunkel, W.; *et al.* (1987). *Supernova 1987A in the Large Magellanic Cloud.* IAU Circular. **4316**: 1.

[51] Martin Bauer, Mathias Heiles, Matthias Neubert, Andrea Thamm (2017). *Axion-Like Particles at Future Colliders.* arXiv:1808.10323 [hep-ph]

[52] E. Armengaud *et al.*, JCAP **1311**, 067 (2013) [arXiv:1307.1488 [astro-ph]].

[53] G. G. Raffelt, Lect. Notes Phys. **741**, 51 (2008) [arXiv:hep-ph/0611350].

[54] R. Essig, R. Harnik, J. Kaplan and N. Toro, Phys. Rev. D **82**, 113008 (2010) [arXiv:1008.0636 [hep-ph]].

[55] J. P. Lees *et al.* [BaBar Collaboration], Phys. Rev. Lett. **113**, no. 20, 201801 (2014) [arXiv:1406.2980 [hep-ex]].